



Journal of Biomedical
Materials Research
Part B: Applied Biomaterials

A 3D printed hydrogel to promote human keratinocytes spheroid-based growth

| | |
|-------------------------------|---|
| Journal: | <i>Journal of Biomedical Materials Research: Part B - Applied Biomaterials</i> |
| Manuscript ID | JBMR-B-22-0452.R1 |
| Wiley - Manuscript type: | Research Article (Direct Via EEO) |
| Date Submitted by the Author: | 15-Nov-2022 |
| Complete List of Authors: | <p>Rocha, Tânia; University of Porto Faculty of Medicine, Biomedicine Teixeira, Ana ; Institute of Science and Innovation in Mechanical and Industrial Engineering, Mechanical Engineering; University of Porto Faculty of Engineering, Mechanical Engineering Guerreiro, Susana; University of Porto Institute for Research and Innovation in Health Sciences; University of Porto Institute of Molecular Pathology and Immunology; University of Porto Faculty of Nutrition and Food Sciences André, António ; Institute of Science and Innovation in Mechanical and Industrial Engineering, Mechanical Engineering; University of Porto Faculty of Engineering, Mechanical Engineering Martins, Pedro; ARAID; Institute of Science and Innovation in Mechanical and Industrial Engineering, Mechanical Engineering Ferreira, João; University of Porto Faculty of Engineering, Mechanical Engineering; Institute of Science and Innovation in Mechanical and Industrial Engineering Negrão, Rita; University of Porto Faculty of Medicine, Biomedicine; CINTESIS</p> |

SCHOLARONE™
Manuscripts

1. Title page

A 3D printed hydrogel to promote human keratinocytes' spheroid-based growth

Running head- 3D printed hydrogel to promote keratinocytes spheroids

Tânia Rocha^{1*}, Ana Margarida Teixeira^{2,3}, Susana G. Gomes^{5,6,7}, António André^{2,3}, Pedro Martins^{3,4}, João Ferreira^{2,3*†}, Rita Negrão^{1,8*}

1-Department of Biomedicine, Biochemistry Unit, Faculty of Medicine, University of Porto, 4200-319 Porto, Portugal;

2-Department of Mechanical Engineering, Faculty of Engineering, University of Porto, 4200-465 Porto, Portugal;

3- Institute of Science and Innovation in Mechanical and Industrial Engineering, 4200-465 Porto, Portugal;

4- Aragonese Foundation for Research and Development (ARAID), Aragón Institute of Engineering Research (i3A), University of Zaragoza, Aragón, Spain;

5-Institute for Research and Innovation in Health (i3S), University of Porto, 4200-135 Porto, Portugal;

6-Institute of Molecular Pathology and Immunology of the University of Porto-IPATIMUP, 4200-135 Porto, Portugal;

7 -Faculty of Nutrition and Food Sciences, University of Porto, 4150-180 Porto, Portugal;

8- CINTESIS @ RISE - Center for Health Technology and Services Research, 4200-319 Porto, Portugal.

*These authors contributed equally to the work

†Corresponding author:

Name: João Pedro Sousa Ferreira

Address: Rua Dr Roberto Frias, 4200-465, Porto

Telephone: +351225081400

Email: j.ferreira@fe.up.pt

FAX: +351225081400

Work done in:

Department of Biomedicine, Faculty of Medicine, University of Porto - Alameda Prof. Hernâni Monteiro, 4200-319 Porto, Portugal; And Institute of Science and Innovation in Mechanical and Industrial Engineering - Rua Dr. Roberto Frias 400, 4200-465 Porto, Portugal

2. Abstract and key terms

Abstract

Tissue engineering uses cells and biomaterials to develop bioartificial tissue substitutes for different purposes. For example, although several skin models have been developed for pharmaceutical and cosmetic research and skin wound healing, there are few studies on 3D cultures of keratinocytes in 3D printed scaffolds.

So, this work aimed to develop a 3D-printed hydrogel scaffold to promote human keratinocyte growth. Mesh 3D scaffolds were printed using an extrusion-based method with a 20% gelatin/ 5% alginate hydrogel, where HaCaT cells were cultured for seven days.

Scaffolds kept their structure for over one week, and their stiffness only decreased after seven days, showing good mechanical and structural characteristics and biodegradability (27% weight lost). Viable keratinocytes (MTT assay) are aggregated into spheroids, a 3D model capable of mimicking in vivo cell properties and phenotypes. Spheroids were formed on 47% of scaffolds pores and grew over time, showing promising cell proliferation. F-actin staining showed cells' irregular and interconnected shapes and organization over time.

This method offers an easy and inexpensive solution for keratinocyte spheroid formation, which may be helpful in tissue engineering as a cell delivery system, for pharmacological or basic research, or wound healing medical applications.

Key terms: Tissue engineering, biomaterials, alginate, gelatin, skin, regeneration, wound healing, HaCaT

3. Introduction

Introduction

Tissue engineering is a biomedical engineering field that combines cells and biomaterials to replace or regenerate tissues [1]. Biomaterials can be used to reconstruct damaged tissue, in wound healing, and as a cell or drug delivery system [2,3]. However, as tissues have different architectural structures and extracellular matrix (ECM) properties, biomaterials should mimic the characteristics of these tissues, allowing cell attachment, migration and proliferation, and enabling the diffusion of nutrients and waste products [1,2]. Tissue engineering often involves scaffolds where cells are seeded and their growth stimulation to form viable and functional tissues for medical purposes [1,2], like skin [4], bone, or cartilage regeneration [5]. It has also been used to design in vitro models of healthy or pathological tissues and organs for cosmetic and drug tests, to evaluate new therapies and investigate phenomena regulating disease onset and progression [1]. For example, there are skin models for psoriasis (TESTSKIN™), melanoma and infection [4].

3D cell culture systems have been extensively studied, especially in tissue engineering, because cellular properties and phenotypes are closer to those observed in vivo when compared to 2D cell culture systems [5]. Organoids and spheroids are 3D cell culture models where cells grow in complex systems closest to physiological and pathological ones and are of great interest and potential in disease models and regenerative medicine [5]. Interestingly enough, Aasen T et al., [6] reprogrammed keratinocytes from human skin biopsies and single human hairs to pluripotency cells, that then differentiate again forming a stratified epidermis in 7 days, developing a very interesting model for tissue reepithelization that deserve to be explored for patient-specific therapy. Alginate is a natural biomaterial for biomedical applications due to its biocompatibility, low toxicity, and crosslinking ability by adding divalent cations such as Ca^{2+} [3]. However, alginate lacks cell-adhesive ligands, so it is often mixed with other biomaterials, such as gelatin, to improve cell adhesion and differentiation [7]. Alginate has also been used for many years as a dressing for highly exuding wounds, ulcers, surgical incisions, and infected wounds [8]. Some commercially available solutions include Algicell™ (Derma Sciences), AlgiSite M™ (Smith & Nephew), and Tegagen™ (3M Healthcare)[3]. These dressings are helpful because they create a moist wound environment, are highly absorptive, nonadherent, biodegradable, and can prevent microbial contamination [7]. The application

3. Introduction

of alginates to skin graft donor sites also results in significantly better healing and reduced pain compared to paraffin gauze controls [9]. Gelatin can also stimulate cell differentiation and proliferation and promote wound healing [10].

Different methods have been described to create scaffolds. For example, computer-assisted design (CAD) and manufacturing (CAM) techniques allow more precise control of porosity and shape. They are faster and more reproducible than conventional gas foaming, melt molding, and freeze-drying techniques [2]. The scaffolds can be created using extrusion-based printing, fused deposition modeling, or selective laser sintering [11]. Extrusion-based systems print the biomaterial layer by layer through a micro-nozzle in the form of continuous filaments through continuous extrusion force [11]. Different biomaterials can be used for this purpose. However, hydrogels are attractive options because their mechanical properties can be adjusted, they are biocompatible and they can be hydrated, similarly to biological tissues, while remaining insoluble and maintaining their 3D structure [12]. Hydrogels are matrixes of hydrophilic polymers that absorb large amounts of water, facilitating the transport of nutrients and oxygen and removing waste products. They also present bioactive stimuli that can influence cellular processes [12]. Different properties like structure, porosity, and biodegradability can influence cell growth [13], so it is essential to study and design new scaffolds and biomaterials to sustain these 3D cell culture systems.

The skin is the largest organ of the human body and has a fundamental role as a protective barrier and immune organ. It also plays a vital role in body temperature regulation and perception of stimuli. The epidermis is the outermost layer of the skin, and keratinocytes, the predominant cells in this skin layer, are responsible for the production of keratin used as a protective skin barrier. They are essential in wound healing re-epithelialization processes [14,15] and can increase their replication rate during inflammation, disease, or injury [16]. When the skin is damaged, it is essential to repair and restore its functions and prevent complications [17]. Although several skin models have been developed, like Skinethic™, Episkin™, and Epiderm™, for both in vivo and in vitro applications for wound healing, disease models and pharmacological and basic research [2], there are still few studies on 3D cultures of keratinocytes in 3D printed scaffolds.

We hypothesize that human keratinocytes can grow and proliferate in 3D-printed alginate-based scaffolds. To test this hypothesis, we applied MTT and Phalloidin assays on human

3. Introduction

1
2
3 keratinocytes seeded in these hydrogels, along with the biodegradability evaluation and
4 quantification of macroscopic mechanical properties under compression. Our cell viability
5 results show the formation of spheroids and their continuous growth over a week.
6
7 Furthermore, the hydrogel scaffolds had a macroscopic stiffness of the same order of
8
9 magnitude as skin and sustained their structure over a week.
10
11
12
13
14
15
16
17
18
19
20
21
22
23
24
25
26
27
28
29
30
31
32
33
34
35
36
37
38
39
40
41
42
43
44
45
46
47
48
49
50
51
52
53
54
55
56
57
58
59
60

For Peer Review

4. Materials and Methods

Materials and Methods

1. Hydrogel preparation and scaffold printing

The hydrogel was a mixture of 20% of gelatin and 5% of alginate, and it was prepared using a previously described method [18]. Briefly, 2g of gelatin (Merck, Germany) was dissolved in 10 mL of sterile phosphate buffer saline (PBS) at 60°C. Then 0.5g of sodium alginate (MP Biomedicals, Portugal) was added, and the mixture was stirred and heated at 60°C until a uniform solution was obtained. To remove air bubbles, the hydrogel was centrifuged three times at 2600 *g* for 5 min and one more time, if necessary. The hydrogel was reheated at 60°C between each centrifugation. It was then aspirated with a 5 ml syringe (dicoNex, France) and transferred to 3 ml cartridges with an adapter (Cellink, Sweden). Finally, a sterile solution of 50 mM calcium chloride dihydrate (Merck, Germany) was prepared and added to 3 ml cartridges using the same method so that it could also be dispensed at the time of printing. The scaffolds were printed using the INKREDIBLE+ bioprinter (Cellink, Sweden). The G-code used for this printing was automatically generated by a parameterized script written in Python3, allowing rapid iteration and testing. Before starting the printing process, all material was disinfected with 70% ethanol, and the printer airflow was set at maximum speed to avoid potential contamination. The hydrogel-filled cartridge was loaded in the printing head (PH) 1 spot with a 27-gauge (210 μm) nozzle, and it was set at a temperature of 37°C and a pressure of approximately 100 kPa. In the cartridge with the CaCl_2 solution, a 22-gauge nozzle (410 μm) was used, and it was loaded in the PH2 at room temperature and with a pressure of 2 kPa. The scaffolds were then printed onto a 12-well cell culture plate. Each structure consisted of a layer-by-layer printed mesh (Fig. 1), with 15 columns and 15 lines, for a total of 5 layers. The line width was set to 350 μm , and the distance between each printed line was set to 500 μm and will be referred to as "pore" from now on (Fig. 1b). In total, the scaffold side had a size of 12,25mm. As each scaffold was printed, approximately 500 μl of CaCl_2 was dispensed from the second printing head (PH2) over each structure so that the time between the end of the impression and the crosslinking of the scaffold was uniform between all, without the need to open the printer door, therefore avoiding contamination.

4. Materials and Methods

[Figure 1 around here]

2. Scaffold sterilization and coating

The scaffolds were then transferred to a new sterile 12-well plate inside a laminar flow hood, washed with sterile Tris buffer saline solution (TBS, Sigma, Portugal) three times, and sterilized for 20 minutes with UV radiation. In order to create a gelatin coating on the structures and improve cell adhesion, scaffolds were covered with 500 μ l of sterile 0.2% gelatin solution and incubated for 15 min at 37°C. Finally, they were transferred to sterile 24-well plates to maximize the area in contact with the cell suspension and to decrease scaffold oscillations inside the well. Cell seeding was performed in these coated scaffolds.

3. Scaffold pore size

Scaffolds were photographed (Motic AE31E, Spain), and 7 random pores from each day (3rd and 7th day) were chosen. Three pore size measurements were performed on each pore using ImageJ software® (National Institute of Health, USA). During the scaffold printing the line width was set to 350 μ m, and the distance between each printed line was set to 500 μ m and is referred to as "pore" along the manuscript. For simplicity, we also refer "porosity" to the "holes" of the scaffold and not to the porosity of the scaffold matrix.

4. Degradation assay

To test scaffold degradation, they were weighed on the day of print (day zero) and the 3rd and 7th days. Scaffold weight loss was calculated in percentage on day 3 and 7, compared to day 0. Between weighings, the scaffolds were maintained in a cell culture medium at 37°C in the cell incubator and dried as much as possible before each weighing (KERN 770, Germany).

5. Mechanical tests

Mechanical tests were conducted at room temperature under displacement control with a flat-ended circular indenter of 5 mm diameter. A 10N S-beam load cell (Applied Measurements, UK), threaded with the indenter, was connected to an actuator with a load capacity of 12 kg and a resolution of 3.05×10^{-4} mm. Both indentation load P and indenter's position z were acquired at 50 Hz. A 0.02 N preload was applied to ensure complete contact between the surfaces of the sample and the indenter. Before testing, each sample was

4. Materials and Methods

subjected to 3 preconditioning cycles at 5 mm/min with an amplitude of 0.3 mm to remove any internal stress accumulation that could arise from sample preparation. Then, ten cycles of 1mm at 5mm/min were applied followed by a stress relaxation test of 3min after ramping to 1.5mm at 30 mm/min (Fig. 2a).

The stress and strain values were obtained from the recorded force-position data as $\sigma = P/(\pi a^2)$ and $\varepsilon = (z - z_0)/z_0$, with a being the radius of the loaded area and z_0 is the sample thickness. As flat circular indenter contact a flat surface, a remains constant during contact. The apparent Young's modulus of the hydrogel was then estimated as [19–22]

$$E = 2 \frac{a(1 - \nu^2)\sigma}{z_0 \varepsilon},$$

The Poisson's ratio ν was set to 0.5 due to the incompressibility of the hydrogel (high water content). We calculated E in the first (E1) and second (E2) half of each cycle loading curve. For each group (days after printing), the stress-strain curves were averaged using the experimental data from three samples. The mean (per day after printing) stress-strain curve was used to estimate Young's modulus.

6. Keratinocytes cell culture

HaCaT cells (CLS, Germany) were cultured in Dulbecco's Modified Eagles's Medium (DMEM, CLS, Germany) supplemented with 10% fetal bovine serum (FBS, Sigma-Aldrich, Portugal) and 1% penicillin/streptomycin (Sigma-Aldrich, Portugal) (complete DMEM) at 37 °C and 5% CO₂ and collected by trypsinization with 0.25% trypsin-EDTA solution (Sigma-Aldrich, Portugal). The cell medium was changed every three days. 4×10^5 Cells were seeded on each scaffold. The scaffolds with HaCaT cells were maintained in complete DMEM and cell culture conditions for 3 and 7 days. HaCaT cells were also cultured in 24-well plates, without scaffolds, in the same conditions.

7. Viable cell labeling

To identify viable cells in the scaffold, under microscope observation, the 3-(4,5-dimethylthiazol-2-yl)-2,5-diphenyltetrazolium bromide (MTT, Sigma-Aldrich, Portugal) assay was used. The formation of a purple formazan inside cells indicates the presence of viable

4. Materials and Methods

cells. On days 3 and 7, the scaffolds were transferred to different 24-wells plates to avoid labeling cells that were not adherent to the scaffold. Then, 500 μ l of cell culture medium and 100 μ l of 5mg/ml MTT were added and cells were incubated at 37°C for 2 hours. After that, scaffolds with HaCaT cells were analyzed and photographed using an inverted optical microscope (Motic AE31E, Spain).

8. Measurement of spheroid size

Spheroids observed after MTT staining were also used for nucleus and total diameter determination at 3rd and 7th days. At least six randomly stained spheroids were photographed (Motic AE31E, Spain), and three diameter measurements were performed on each spheroid using ImageJ software® (National Institute of Health, USA).

9. Quantification of spheroid filled pores

The number of pores of the scaffolds occupied with spheroids was compared to the total number of pores in each scaffold, which was 196 in total (%). Spheroids were easily observed as white spots present in the scaffolds. Therefore, scaffolds with a minimum of 8 white spots per quadrant were selected for quantification. The spheroids were counted on days 3 and 7 using an inverted optical microscope (Nikon ECLIPSE 50i, UK).

11. Cytoskeleton labeling

Actin filaments (F-actin) from the cytoskeleton of HaCaT cells growing on scaffolds were labeled with Alexa Fluor™ 488 Phalloidin A12379 (Invitrogen, Thermofisher, Portugal), at the 3rd and 7th days of cell culture.

HaCaT cells were also seeded on glass coverslips, previously coated with 0.2% gelatin, in 24-well plates, as a control of 2D culture growth.

Briefly, cells were fixed in 4% paraformaldehyde in TBS for 10 minutes at room temperature, rinsed with TBS and then cells were stained by incubation with Alexa Fluor™ 488 Phalloidin A12379 in 1% BSA for 20 min, rinsed three times quickly in TBS and mounted in glycerol:PBS to the cover slip. Cells were also stained with 1 μ g/ml 4',6-Diamidine-2'-phenylindole dihydrochloride (DAPI, Roche, Portugal) for 10 min, at room temperature.

4. Materials and Methods

Images were examined and captured under a fluorescence microscope (Zeiss Axio Imager Z1, Carl Zeiss, Germany) with 495 nm (Alexa Fluor™ 488) and 340/380 nm (DAPI) excitation filters and processed with the Carl Zeiss™ AxioVision program version 4.8.

12. Calculations and statistics

Data are expressed as arithmetic mean \pm standard deviation (SD) except for indentation values E1 and E2 where the standard error of the mean (SEM) was used. Welch's t-test was used for comparisons between the two groups. Differences were considered significant at a confidence interval of 95% whenever $p < 0.05$, and the following symbols were used to mark significance levels: $p^* < 0.05$, $p^{**} < 0.01$, $p^{***} < 0.001$. The sample size (n) corresponds to the number of independent measurements. All the statistical analysis was performed in Python using NumPy, Pandas, SciPy, and Seaborn packages [23,24].

5. Results

Results

Scaffold properties

The structural and mechanical properties of the scaffolds were evaluated. The mean scaffold pore size was $444 \pm 25 \mu\text{m}$ ($n=7$) on day 3 and $443 \pm 47 \mu\text{m}$ ($n=7$) on day 7.

Printed scaffolds were maintained in cell culture conditions for a maximum of 7 days, and their properties were evaluated on days 3 and 7. All tested scaffolds lost weight during the week. The loss was $23 \pm 2 \%$ ($n=12$, $p=0.0008$) at day 3 and $27 \pm 3 \%$ ($n=12$, $p=0.001$) after 7 days when comparing to day 0 (Fig. 2b). No significant differences in weight loss between day 3 and day 7 were found ($p=0.176$).

Regarding mechanical properties, E1 characterizes the stiffness for low compressive strains, while E2 describes higher strain values. The indentation tests showed that E1 was significantly higher in day 0 ($22 \pm 2 \text{ kPa}$, $n=2$) when compared to day 7 ($10 \pm 2 \text{ kPa}$, $n=4$) ($p=0.031$, Fig.2c) and in day 3 ($17 \pm 1 \text{ kPa}$, $n=3$) when compared to day 7 ($p=0.014$). No significant differences were found between day 0 and day 3 ($p=0.162$). The obtained E2 value was $33 \pm 2 \text{ kPa}$ ($n=2$) at day 0, $26 \pm 3 \text{ kPa}$ ($n=3$) at day 3, and $21 \pm 5 \text{ kPa}$ ($n=4$) at day 7 (Fig.2c). Although E2 results have a similar profile, tending to decrease from day 0 to day 7, no significant differences were found between different days.

Scaffold resilience upon deformation was also evaluated by their relaxation/recovery ability in the relaxation tests. The observed results were $44 \pm 1 \%$ ($n=3$) on day 0, $32 \pm 11 \%$ ($n=3$) on day 3 and $32 \pm 3 \%$ ($n=5$) on day 7 (Fig.2d). Relaxation significantly decreased from day 0 to day 7 ($p=0.0006$, Fig.2d).

[Figure 2 around here]

Spheroid evolution

It was observed that when HaCaT cells were seeded on the scaffolds, they did not grow in a monolayer covering the scaffold structure. Instead, they organized themselves in spheroid structures (Fig. 3 and 4).

5. Results

When compared to the total number of pores in a scaffold, which was 196, the percentage of pores that were occupied by spheroids was 49% ($n=3$) on day 3. This number decreased slightly to 47% ($n=3$) on day 7 (Fig.3a). This decrease was not statistically significant ($p=0.77$).

Spheroid total size significantly increased from day 3 to day 7 ($p=0.01$, Fig.3b) while nucleus size decreased from day 3 to day 7 ($p=0.009$, Fig.3b). On day 3, the average total size was $270 \pm 11 \mu\text{m}$ ($n=7$) and on day 7 it was $342 \pm 19 \mu\text{m}$ ($n=6$), showing a growth of about $72 \mu\text{m}$. This size difference can also be seen in Fig.3c and Fig.3d. On day 3, the average nucleus size was $150 \pm 6 \mu\text{m}$ ($n=7$) and on day 7 it was $120 \pm 8 \mu\text{m}$ ($n=6$),

Figure 3c shows a scaffold on the 3rd day, with spheroids inside its pores (the red square illustrates the limits of a pore). These spheroids do not fill the entire pore and are not perfectly spherical (Fig.3c and 3e). In contrast, spheroids on day 7 are larger, rounder, and able to fill the entire pore (Fig.3d and 3f).

[Figure 3 around here]

Cell viability

The viability of cells inside these spheroids was evaluated by MTT assay. After incubating the scaffold with MTT, a formazan accumulates inside viable cells, indicated by a purple color as seen in spheroids images shown in figure 4.

Figure 4a, 4c, 4e, and 4g show spheroids on day 3 with different magnifications. A spheroid core with intense purple color and cells around it can be seen, also labeled with purple, indicating viable cells. Figure 4b, 4d, 4f and 4h show spheroids on day 7 with different magnifications. The core of the spheroid on day 7 is smaller, although the entire spheroid is larger when compared to the spheroid on day 3, as already described in figure 3b. Nevertheless, the core and surrounding cells, which are more abundant, are also marked with purple color, indicating viable cells. These figures also show differences in the size and shape of the 3rd and 7th day spheroids.

[Figure 4 around here]

5. Results

Cell cytoskeleton

HaCaT cells cultured on gelatin-coated coverglass were labeled using phalloidin (green) and DAPI (blue) and the results obtained at the 3rd (Fig. 5a) and 7th (Fig. 5b) days are shown in figure 5. These images show 2D cell shapes through F-actin labeling. Cells are not round and quiescent; they show irregular and interconnected shapes.

Spheroids were labeled using the same protocol; the results are also shown in figure 5. Although cells are organized in 3D spheroid structures at both 3rd (Fig. 5c, 5e and 5g) and 7th (Fig. 5d, 5f and 5h) days of culture, as already mentioned above, cells are not quiescent, showing irregular shapes, particularly in the middle of spheroids (Fig. 5c and 5d). Fig. 5g and 5h show the same spheroids from Fig. 5e and 5f, respectively, but in combination with a white light filter to show the scaffold's pore structure. These images also show a core of aggregated cells that form a spherical structure in the middle of the spheroid and many loose cells in the periphery of these 3D structures. This arrangement was seen on the majority of spheroids on both days.

[Figure 5 around here]

6. Discussion

Discussion

The skin is the largest organ in the human body and has fundamental functions as a physical barrier and immune organ. It can be damaged by, for example, cuts, burns, pressure, or chemicals and impaired wound healing can lead to complications such as infections, neuronal damage and pain [17]. Tissue engineering can be critical to promote wound healing, especially when the affected area is too large to be treated with conventional techniques [4]. Scaffolds are often used since they enable the formation of viable tissues from 3D cell cultures, which can be used as implants to repair or replace damaged tissues [5].

Our results demonstrate that scaffolds printed with 20% gelatin/5% alginate hydrogel could promote a viable growth of keratinocytes into spheroids within 7 days. Such a model allows the study of keratinocytes under 3D growing conditions and can potentially be applied as a cheap and fast carrier of keratinocytes for skin lesions treatment. Spheroids are an important 3D cell culture model. They are self-assembling and complex spherical cell aggregates with cell-cell and cell-matrix interactions that mimic in vivo tissues and their physiological activity [5]. 2D cell cultures, where cells grow in a monolayer attached to a plastic or glass surface, are the most known and used methods due to their simplicity, low cost, and reproducibility [5,13]. However, 2D cultured cells manifest different behavior and properties than in vivo cells as they do not mimic their 3D environment. For example, cells cultured two-dimensionally can be stretched, resulting in cytoskeletal rearrangements and artificial polarity, limiting their interactions, presenting physical and physiological differences, modified biochemical profiles, bioactivity, and drug resistance [5,13,25]. In contrast, 3D cell cultures, like spheroids, mimic the geometry of three-dimensional tissues more accurately. Therefore cells present a profile closer to that shown in vivo [13], having many applications for tissue engineering[5].

Spheroids can be fabricated using various methods and the same culture medium as 2D cultures. Scaffold-free approaches produce spheroids alone and scaffold approaches, as used in this study [5]. An essential advantage of scaffolds is the mechanical reinforcement provided to the cells [5].

Although we tried to promote the adhesion of cells to the scaffold using a large proportion of gelatin in our hydrogel and using a 0.2% gelatin coating, cell-cell interactions seemed stronger, showing the predominant spheroid formation and only a few isolated cells growing

6. Discussion

1
2
3 along the scaffold [26], in contrast to results shown in a previous study using a 20% gelatin/4%
4 alginate hydrogel [13]. This could be explained by some denature of gelatin structure as it was
5 subjected to high temperatures to avoid contamination during scaffold preparation.
6
7

8
9 The lack of studies regarding 3D keratinocytes cell cultures using 3D printed scaffolds able to
10 promote cell growth and other desired properties such as cell adherence, migration and
11 interactions turned relevant to develop a 3D-printed hydrogel scaffold able to promote the
12 growth of human keratinocytes.
13
14

15
16 We used the HaCaT cell line, a non-tumorigenic monoclonal cell line of spontaneously
17 immortalized human keratinocytes, as it has been proposed as a model for the study of
18 keratinocytes functions. They have some advantages compared to fresh human keratinocytes
19 as they are adapted for long-term growth without additional growth factors, exhibit normal
20 morphogenesis and express all significant surface markers and functional keratinocytes
21 activity, retaining the ability to reconstitute a well-structured epidermis after in vivo
22 transplantation [27].
23
24

25
26 Scaffolds were produced using a 3D bioprinter (INKREDIBLE+ by CELLINK) as previously
27 described [11]. This device uses a pneumatic-based system to extrude the hydrogel through
28 a thin nozzle, with precise positioning of a moving printing head in X, Y, and Z. This technology
29 is fast, reproducible and highly computer controllable, thus allowing the precise printing of
30 3D structures. These may be porous grid structures that promote the circulation of nutrients
31 and metabolites [16], like in this study.
32
33

34
35 The G-code used for printing was automatically generated by a python script, allowing to
36 easily adjust all scaffold measurements and precise control of porosity and shape. It also
37 enabled printing in multiwell plates and optimizing the printing process, avoiding unnecessary
38 and time-consuming movements.
39
40

41
42 The printing head temperature was set to 37°C to facilitate hydrogel extrusion. However, we
43 had some printing precision and reproducibility issues, likely because the printer's platform
44 was at room temperature, and we worked with a temperature-sensitive hydrogel. The printer
45 was also under non-sterile conditions, so scaffolds had to be posteriorly sterilized using UV
46 radiation, a method shown to have promising results in terminal sterilization of alginate
47 scaffolds without affecting their mechanical properties [28] or dehydrating the scaffolds like
48 ethanol. Other sterilization processes that do not induce significant changes in the properties
49 of the scaffolds have been suggested by Augustine et al. [29]. The sterilization by gamma
50
51
52
53
54
55
56
57
58
59
60

6. Discussion

radiation above 35 kGy of polycaprolactone scaffolds eliminated the presence of microorganisms and did not modify fibroblasts growth, proliferation and adhesion to the scaffold. On contrary, cells seem to grow better on gamma radiation sterilized material. We used a hydrogel with 20% gelatin and 5% alginate, similar to a previously tested hydrogel for mouse bone mesenchymal stem cell growth [13]. Both alginate and gelatin promote wound healing [8,10] and this combination has been described for biomedical applications including the skin [7] and has also been attempted because of its chemical similarity to the ECM [13]. The printed scaffolds were mesh structures with a total of 196 pores with 500x500 μm each and a diagonal of 707 μm . On images obtained after printing, some pores appeared rounder, so we measured the most significant dimensions of each one, equivalent to their diagonals. The mean scaffold pore size was 444 μm on 3rd day and 443 μm on the 7th day, about 63% of the initially designed size, but it didn't change over 1 week, which shows good structural integrity. Scaffolds decreased their overall size after crosslinking, and the hydrogel lines may have gotten more prominent due to water absorption, explaining the smaller pore size compared to the design [13].

The tests to evaluate scaffold structural integrity and properties during one week revealed that scaffolds kept their basic structure and design after one week, as seen on microscopic images, but some of their properties changed. For example, scaffolds lost 23% of their weight on day 3 and 27% on day 7, when maintained in cell culture conditions, suggesting that this loss occurs in the first days as the decrease observed between the 3rd and 7th days was not significant. Furthermore, the degradation after 7 days was similar to previously reported results for a 20% gelatin/4% alginate hydrogel. However, after 3 days in our study, the degradation was approximately twice the value of the previous results [13]. Overall, this hydrogel showed good biodegradability, which could be due to its chemical structure, the incubation temperature or the transport processes of various chemicals such as water and ions (H^+ and OH^-) [30].

Indentation tests showed a decrease of scaffolds stiffness throughout the week. However, the scaffolds stiffness for low compressive strains (E1) only decreased significantly on day 7 and for higher strain values (E2) the change was not significant, which shows good mechanical strength properties. This is a result of scaffold degradation and consequent loss of resistance. Scaffolds also showed a low recovery ability with low relaxation values, meaning they have low resilience upon deformation, which could be associated with scaffold stiffness [31]. After

6. Discussion

7 days, their relaxation decreased significantly (12%) compared to the first day, possibly due to ionic and covalent crosslinking changes as the scaffolds spent time in the incubator conditions [32].

These mechanical and physical evaluation tests were done in scaffolds without cells to facilitate their manipulation. However, this might have changed the results, even if slightly, as it has been demonstrated that cells may have a role in crosslinking and degradation processes, affecting scaffold properties [3]. Therefore, in future studies, scaffolds should also be analyzed using different methods like scanning electron microscopy to study their structural characteristics over time.

Our scaffolds promoted spheroid formation and growth. About 47% of all the pores were filled with a spheroid on day 3 and 45% on day 7. Spheroids were significantly larger over one week, showing a growth of about 21% between days 3 and 7, filling a more significant portion of each pore. This indicates that the cells inside these spheroids are viable and in proliferation, which is extremely important in tissue engineering and ensuring proper cell delivery. MTT assay proved the presence of viable cells as a purple color inside cells was observed due to the formazan formed in the 3rd and 7th days, as shown in microscopic images. Accordingly, the results obtained for F-actin labeling, a major cytoskeleton component involved in many cellular processes such as cell division and migration [33], showed that cells in the spheroids are not round and quiescent but rather active and interacting. In phalloidin images, we could see a core of aggregated cells and many loose cells. We do not know if these loose cells mean that they are leaving the spheroid to colonize the scaffold structure or if this was an artifact caused by the washing steps required during the staining protocol. Because of this, spheroid size was measured on MTT assay spheroids, where there was minimal handling of the samples. The imaging was challenging on both MTT and phalloidin methods due to the spheroid's high thickness, resulting in a light-scattering phenomenon that limits light penetration [34]. Therefore, spheroids sectioning or optical clearing methods could be used in the future to obtain better resolution [34].

Since alginate has been used for many years as a wound dressing and shows significant characteristics capable of improving healing, the results herein presented represent a new step in this field as they show that alginate/gelatin scaffolds are attractive supports able to promote human keratinocytes growth into spheroids, that deserve to be better explored as wound dressings able to deliver keratinocytes to promote wound healing. Also, as

6. Discussion

1
2
3 keratinocytes grown in these 3D spheroids structures mimic human tissue properties more
4 accurately than monolayer cell cultures, they may be helpful to study models, and the
5 exploration of their clinical and regenerative utility seems great interest. In future studies,
6 other cell types, such as fibroblasts, could be co-cultured to mimic skin environment and cell
7 interactions and eventually potentiate healing properties even further.
8
9
10
11
12
13
14
15
16
17
18
19
20
21
22
23
24
25
26
27
28
29
30
31
32
33
34
35
36
37
38
39
40
41
42
43
44
45
46
47
48
49
50
51
52
53
54
55
56
57
58
59
60

For Peer Review

7. Acknowledgments

Acknowledgments

National Funds supported this article through FCT - Fundação para a Ciência e a Tecnologia, IP, within CINTESIS, R&D Unit (reference UIDB/4255/2020) and by project CyclicCell - PTDC/EME-APL/1342/2020 financed through FCT/FEDER/MCTES.

We would like to thank Professor António Avelino for his help with microscopic imaging.

The authors declare no conflict of interest.

References

1. Caddeo S, Boffito M, Sartori S. Tissue engineering approaches in the design of healthy and pathological in vitro tissue models. Vol. 5, *Frontiers in Bioengineering and Biotechnology*. 2017.
2. Do AV, Khorsand B, Geary SM, Salem AK. 3D Printing of Scaffolds for Tissue Regeneration Applications. Vol. 4, *Advanced Healthcare Materials*. 2015.
3. Lee KY, Mooney DJ. Alginate: Properties and biomedical applications. Vol. 37, *Progress in Polymer Science (Oxford)*. 2012.
4. Groeber F, Holeiter M, Hampel M, Hinderer S, Schenke-Layland K. Skin tissue engineering - In vivo and in vitro applications. Vol. 63, *Advanced Drug Delivery Reviews*. 2011.
5. Chae SJ, Hong J, Hwangbo H, Kim GH. The utility of biomedical scaffolds laden with spheroids in various tissue engineering applications. *Theranostics*. 2021;11(14).
6. Aasen T, Raya A, Barrero MJ, Garreta E, Consiglio A, Gonzalez F, Vassena R, Bilić J, Pekarik V, Tiscornia G, Edel M, Boué S, Belmonte JCI. Efficient and rapid generation of induced pluripotent stem cells from human keratinocytes. *Nat Biotechnol*. 2008;26(11).
7. Van Vlierberghe S, Dubruel P, Schacht E. Biopolymer-based hydrogels as scaffolds for tissue engineering applications: A review. Vol. 12, *Biomacromolecules*. 2011.
8. Aderibigbe BA, Buyana B. Alginate in wound dressings. Vol. 10, *Pharmaceutics*. 2018.
9. Attwood AI. Calcium alginate dressing accelerates split skin graft donor site healing. *Br J Plast Surg*. 1989;42(4).
10. Ndlovu SP, Ngece K, Alven S, Aderibigbe BA. Gelatin-based hybrid scaffolds: Promising wound dressings. Vol. 13, *Polymers*. 2021.
11. Gu Z, Fu J, Lin H, He Y. Development of 3D bioprinting: From printing methods to biomedical applications. Vol. 15, *Asian Journal of Pharmaceutical Sciences*. 2020.
12. El-Sherbiny IM, Yacoub MH. Hydrogel scaffolds for tissue engineering: Progress and

- challenges. *Glob Cardiol Sci Pract.* 2013;2013(3).
13. Pan T, Song W, Cao X, Wang Y. 3D Bioplotting of Gelatin/Alginate Scaffolds for Tissue Engineering: Influence of Crosslinking Degree and Pore Architecture on Physicochemical Properties. *J Mater Sci Technol.* 2016;32(9).
 14. Rodrigues M, Kosaric N, Bonham CA, Gurtner GC. Wound healing: A cellular perspective. *Physiol Rev.* 2019;99(1).
 15. Klicks J, von Molitor E, Ertongur-Fauth T, Rudolf R, Hafner M. In vitro skin three-dimensional models and their applications. *J Cell Biotechnol.* 2017;3(1).
 16. Weng T, Zhang W, Xia Y, Wu P, Yang M, Jin R, Xia S, Wang J, You C, Han C, Wang X. 3D bioprinting for skin tissue engineering: Current status and perspectives. Vol. 12, *Journal of Tissue Engineering.* 2021.
 17. Nguyen A V., Soulika AM. The dynamics of the skin's immune system. Vol. 20, *International Journal of Molecular Sciences.* 2019.
 18. Giuseppe M Di, Law N, Webb B, A. Macrae R, Liew LJ, Sercombe TB, Dilley RJ, Doyle BJ. Mechanical behaviour of alginate-gelatin hydrogels for 3D bioprinting. *J Mech Behav Biomed Mater.* 2018;79.
 19. Cheng CM, Cheng YT. On the initial unloading slope in indentation of elastic-plastic solids by an indenter with an axisymmetric smooth profile. *Appl Phys Lett.* 1997;71(18).
 20. King RB. Elastic analysis of some punch problems for a layered medium. *Int J Solids Struct.* 1987;23(12).
 21. Oliver WC, Brotzen FR. On the generality of the relationship among contact stiffness, contact area, and elastic modulus during indentation. *J Mater Res.* 1992;7(3).
 22. Sneddon IN. The relation between load and penetration in the axisymmetric boussinesq problem for a punch of arbitrary profile. *Int J Eng Sci [Internet].* 1965 May 1;3(1):47–57. Available from: <https://linkinghub.elsevier.com/retrieve/pii/0020722565900194>
 23. Virtanen P, Gommers R, Oliphant TE, Haberland M, Reddy T, Cournapeau D, Burovski E, Peterson P, Weckesser W, Bright J, van der Walt SJ, Brett M, Wilson J, Millman KJ, Mayorov N, Nelson ARJ, Jones E, Kern R, Larson E, Carey CJ, Polat İ, Feng Y, Moore EW, VanderPlas J, Laxalde D, Perktold J, Cimrman R, Henriksen I, Quintero EA, Harris CR, Archibald AM, Ribeiro AH, Pedregosa F, van Mulbregt P, Vijaykumar A, Bardelli A Pietro, Rothberg A, Hilboll A, Kloeckner A, Scopatz A, Lee A, Rokem A, Woods CN, Fulton C, Masson C, Häggström C, Fitzgerald C, Nicholson DA, Hagen DR, Pasechnik D V., Olivetti E, Martin E, Wieser E, Silva F, Lenders F, Wilhelm F, Young G, Price GA, Ingold GL, Allen GE, Lee GR, Audren H, Probst I, Dietrich JP, Silterra J, Webber JT, Slavič J, Nothman J, Buchner J, Kulick J, Schönberger JL, de Miranda Cardoso JV, Reimer J, Harrington J, Rodríguez JLC, Nunez-Iglesias J, Kuczynski J, Tritz K, Thoma M, Newville M, Kümmerer M, Bolingbroke M, Tartre M, Pak M, Smith NJ, Nowaczyk N, Shebanov N, Pavlyk O, Brodtkorb PA, Lee P, McGibbon RT, Feldbauer R, Lewis S, Tygier S, Sievert S, Vigna S, Peterson S, More S, Pudlik T, Oshima T, Pingel TJ, Robitaille TP, Spura T, Jones TR, Cera T, Leslie T, Zito T, Krauss T, Upadhyay U, Halchenko YO, Vázquez-Baeza Y. *SciPy 1.0: fundamental algorithms for scientific*

- 1
2
3 computing in Python. *Nat Methods*. 2020;17(3).
4
- 5 24. Van Der Walt S, Colbert SC, Varoquaux G. The NumPy array: A structure for efficient
6 numerical computation. *Comput Sci Eng*. 2011;13(2).
7
- 8 25. Sun T, Jackson S, Haycock JW, MacNeil S. Culture of skin cells in 3D rather than 2D
9 improves their ability to survive exposure to cytotoxic agents. *J Biotechnol*.
10 2006;122(3).
11
- 12 26. Nie Y, Xu X, Wang W, Ma N, Lendlein A. Spheroid formation of human keratinocyte:
13 Balancing between cell-substrate and cell-cell interaction. In: *Clinical Hemorheology*
14 *and Microcirculation*. 2020.
15
- 16 27. Colombo I, Sangiovanni E, Maggio R, Mattozzi C, Zava S, Corbett Y, Fumagalli M,
17 Carlino C, Corsetto PA, Scaccabarozzi D, Calvieri S, Gismondi A, Taramelli D, Dell'Agli
18 M. HaCaT Cells as a Reliable in Vitro Differentiation Model to Dissect the
19 Inflammatory/Repair Response of Human Keratinocytes. *Mediators Inflamm*.
20 2017;2017.
21
- 22 28. Stoppel WL, White JC, Horava SD, Henry AC, Roberts SC, Bhatia SR. Terminal
23 sterilization of alginate hydrogels: Efficacy and impact on mechanical properties. *J*
24 *Biomed Mater Res - Part B Appl Biomater*. 2014;102(4).
25
- 26 29. Augustine R, Saha A, Jayachandran VP, Thomas S, Kalarikkal N. Dose-dependent
27 effects of gamma irradiation on the materials properties and cell proliferation of
28 electrospun polycaprolactone tissue engineering scaffolds. *Int J Polym Mater Polym*
29 *Biomater*. 2015;64(10).
30
- 31 30. Lyu SP, Schley J, Loy B, Lind D, Hobot C, Sparer R, Untereker D. Kinetics and time-
32 temperature equivalence of polymer degradation. *Biomacromolecules*. 2007;8(7).
33
- 34 31. You F, Wu X, Chen X. 3D printing of porous alginate/gelatin hydrogel scaffolds and
35 their mechanical property characterization. *Int J Polym Mater Polym Biomater*.
36 2017;66(6).
37
- 38 32. Charbonier F, Indana D, Chaudhuri O. Tuning Viscoelasticity in Alginate Hydrogels for
39 3D Cell Culture Studies. *Curr Protoc*. 2021;1(5).
40
- 41 33. Small JV, Rottner K, Hahne P, Anderson KI. Visualising the actin cytoskeleton. *Microsc*
42 *Res Tech*. 1999;47(1).
43
- 44 34. Costa EC, Silva DN, Moreira AF, Correia IJ. Optical clearing methods: An overview of
45 the techniques used for the imaging of 3D spheroids. Vol. 116, *Biotechnology and*
46 *Bioengineering*. 2019.
47
48
49
50
51
52
53
54
55
56
57
58
59
60

FIGURE CAPTIONS:

Fig. 1 - Scaffold 3D model. (a) Isometric view; (b) Top view; the red square illustrates a pore, the line width is 350 μm and the pore width is 500 μm . Scaffolds size was 12,25 x 12,25 mm^2

Fig. 2 - Scaffolds physical and mechanical properties evaluation (a) Mechanical tests protocol; (b) Scaffold weight loss (%), $p^{***}=0.0008$ when comparing day 0 to day 3 and $p^{**}=0.001$ when comparing day 0 to day 7; (c) Scaffold stiffness (kPa), E1 characterizes the scaffold stiffness for low compressive strains while E2 is for higher strain values, $p^*=0.031$ when comparing E1 day 0 to day 7 and $p^*=0.014$ when comparing E1 from day 3 to day 7; (d) Scaffold relaxation (%), $p^{***}=0.0006$ when comparing day 0 and 7.

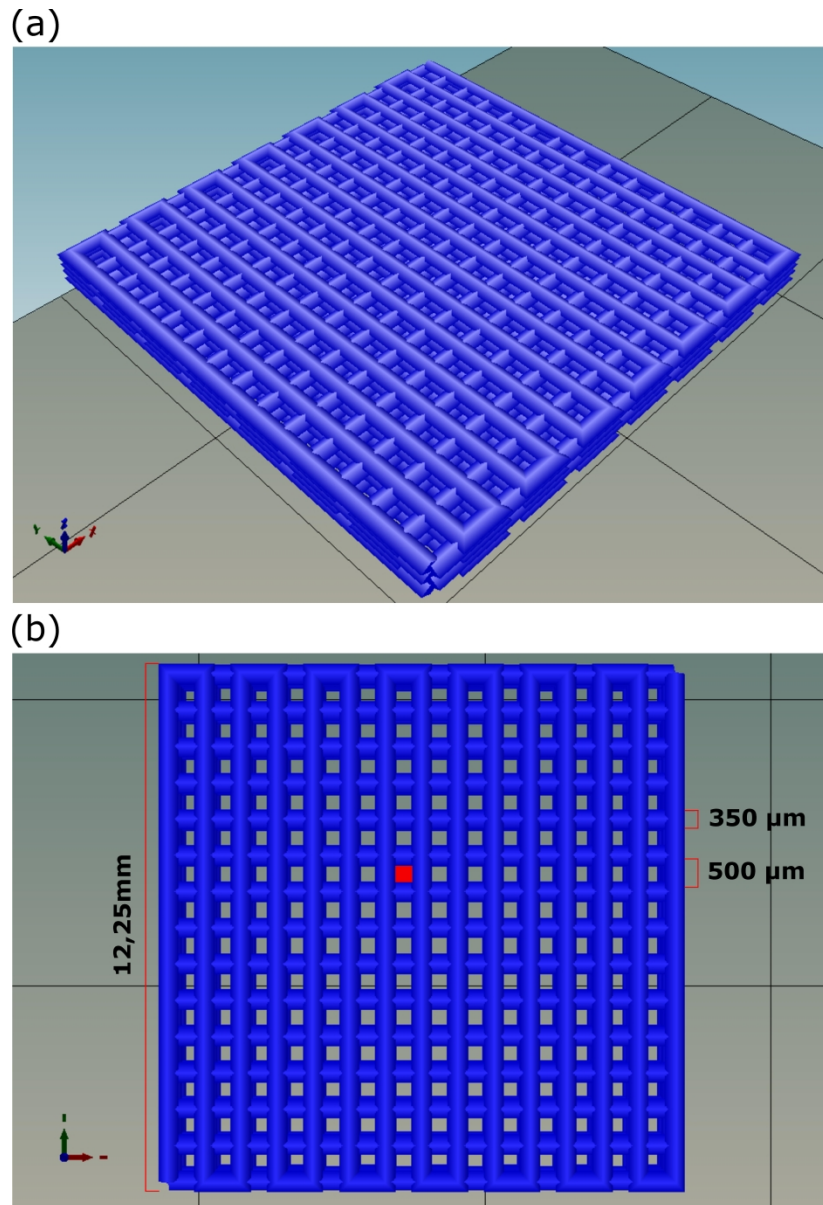
Fig. 3 - Cells organized in spheroids in scaffold pores. (a) Spheroid-filled pores (%) on 3rd and 7th days; (b) Nucleus and spheroid size (μm) on 3rd and 7th days; (c) Scaffold with spheroid-filled pores on 3rd day and (d) on 7th day (The red square illustrates an entire pore; magnification is 40x); (e) Spheroid inside a pore on 3rd day and (f) on 7th day (magnification is 100x).

Fig. 4 – Evaluation of viability of spheroids cells by MTT labeling (a)(c) Spheroid on 3rd day and (b,d) 7th day with 200x magnification; (e,g) Spheroid on 3rd and (f,h) 7th day with 400x magnification;

Fig. 5 – Immunofluorescence observed upon labeling of HaCaT cells and spheroids with phalloidin (green) and DAPI (blue). (a) 2D cell culture on 3rd day and (b) on 7th day; (c) 3rd day spheroid and (d) 7th day spheroid; (e) Spheroid showing a core of cells surrounded by loose cells on 3rd day and (f) on 7th day; (g,h) the same spheroid as seen in Fig.5e and Fig.5f

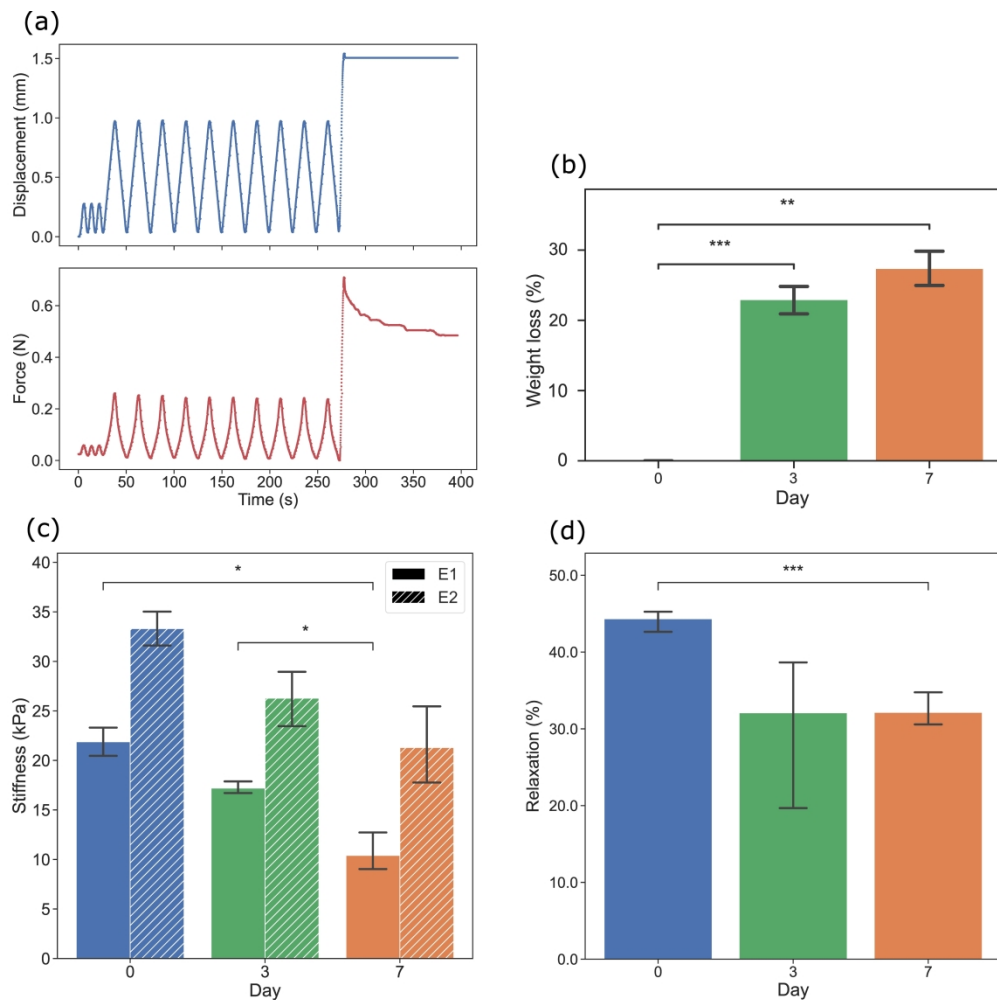
1
2
3 respectively, but photographed with white light, showing the pore's structure. Magnification
4 of 400x in (a) and (b) and 100x on the remaining images.
5
6
7
8
9
10
11
12
13
14
15
16
17
18
19
20
21
22
23
24
25
26
27
28
29
30
31
32
33
34
35
36
37
38
39
40
41
42
43
44
45
46
47
48
49
50
51
52
53
54
55
56
57
58
59
60

For Peer Review



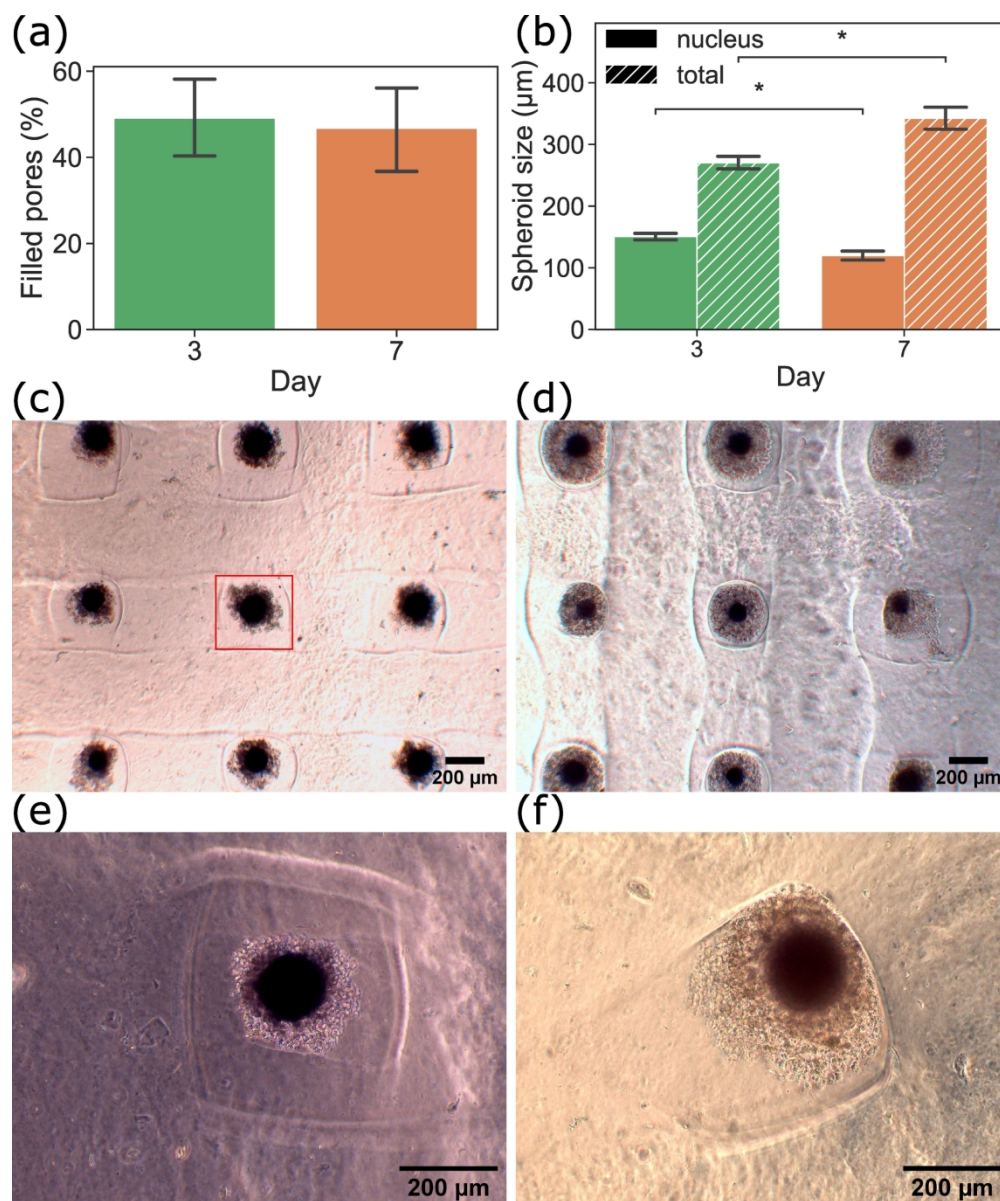
45 Scaffold 3D model. (a) Isometric view; (b) Top view; the red square illustrates a pore, the line width is 350
46 μm and the pore width is 500 μm . Scaffolds size was 12,25 x 12,25 mm²

47
48 251x366mm (600 x 600 DPI)



Scaffolds physical and mechanical properties evaluation (a) Mechanical tests protocol; (b) Scaffold weight loss (%), $p^{***}=0.0008$ when comparing day 0 to day 3 and $p^{**}=0.001$ when comparing day 0 to day 7; (c) Scaffold stiffness (kPa), E1 characterizes the scaffold stiffness for low compressive strains while E2 is for higher strain values, $p^*=0.031$ when comparing E1 day 0 to day 7 and $p^*=0.014$ when comparing E1 from day 3 to day 7; (d) Scaffold relaxation (%), $p^{***}=0.0006$ when comparing day 0 and 7.

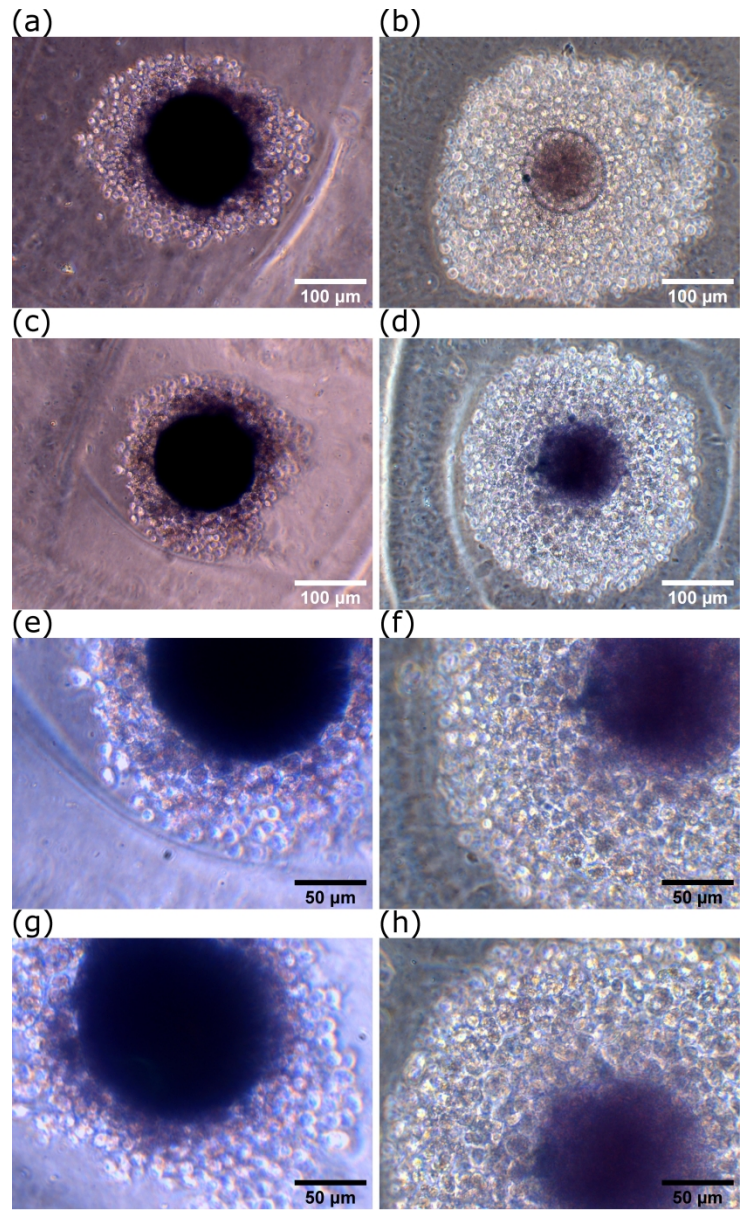
427x424mm (300 x 300 DPI)



Cells organized in spheroids in scaffold pores. (a) Spheroid-filled pores (%) on 3rd and 7th days; (b) Spheroid total and nucleus size (μm) on 3rd and 7th days; (c) Scaffold with spheroid-filled pores on 3rd day and (d) on 7th day (The red square illustrates an entire pore; magnification is 40x); (e) Spheroid inside a pore on 3rd day and (f) on 7th day (magnification is 100x).

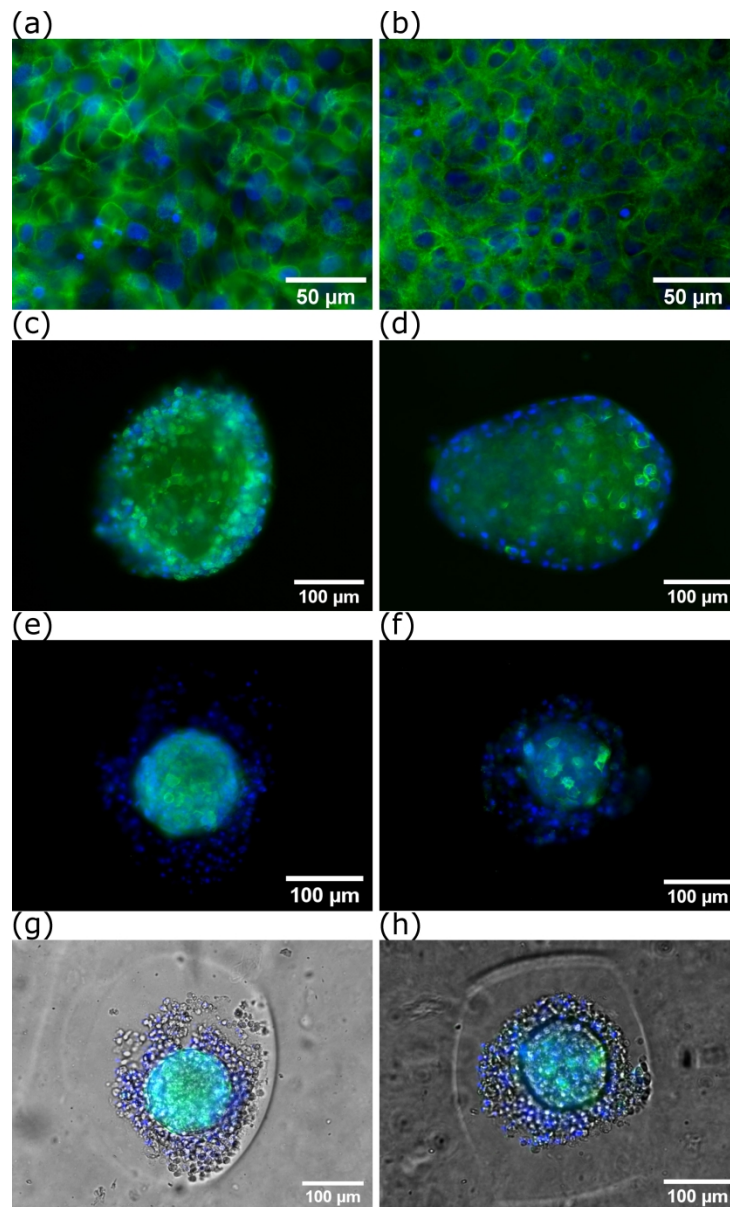
196x232mm (300 x 300 DPI)

1
2
3
4
5
6
7
8
9
10
11
12
13
14
15
16
17
18
19
20
21
22
23
24
25
26
27
28
29
30
31
32
33
34
35
36
37
38
39
40
41
42
43
44
45
46
47
48
49
50
51
52
53
54
55
56
57
58
59
60



Evaluation of viability of spheroids cells by MTT labeling (a)(c) Spheroid on 3rd day and (b,d) 7th day with 200x magnification; (e,g) Spheroid on 3rd and (f,h) 7th day with 400x magnification;

195x322mm (600 x 600 DPI)



Immunofluorescence observed upon labeling of HaCaT cells and spheroids with phalloidin (green) and DAPI (blue). (a) 2D cell culture on 3rd day and (b) on 7th day; (c) 3rd day spheroid and (d) 7th day spheroid; (e) Spheroid showing a core of cells surrounded by loose cells on 3rd day and (f) on 7th day; (g,h) the same spheroid as seen in Fig.5e and Fig.5f respectively, but photographed with white light, showing the pore's structure. Magnification of 400x in (a) and (b) and 100x on the remaining images.

195x322mm (600 x 600 DPI)

1
2
3 Dear Reviewers,
4

5 On behalf of my co-authors I thank you for your time, effort and for the valuable criticism on our
6 manuscript. We appreciate your interest in our results, and your decision to consider our manuscript
7 for publication.
8

9
10 Based on your comments we improved the manuscript by making all the suggested revisions. The
11 point-by-point responses to your comments are given below. We believe that your criticism helped
12 us to significantly improve the quality of our manuscript. All changes and additions we made in the
13 text are highlighted by color in the revised marked version of the manuscript. The page numbers
14 mentioned in our responses below refer to the highlighted (marked) copy of the revised manuscript
15 (MS).
16
17
18

19 Reviewer: 1
20

21 “This manuscript by Rocha et al. reported a gelatin/alginate hydrogel through 3D printing to
22 promote HaCaT cell spheroids formation. A 3D 20% gelatin/5% alginate porous hydrogel scaffold was
23 prepared with good mechanical and biodegradability. The authors showed that HaCaT cells can form
24 spheroids on the hydrogel with good viability and interconnected shape. This is an interesting study
25 for keratinocyte spheroid formation to mimic in vivo conditions.”
26
27

28 We thank the reviewer for the encouraging remarks on our manuscript.
29
30

31 “The logic flow of introduction is not clear. Such as paragraphs 1 and 5 are the same topic, tissue
32 engineering. Paragraphs 2 and 3 discuss alginate for hydrogel preparation, but gelatin is discussed
33 separately in these two paragraphs, the reviewer suggests combining gelatin parts. The reviewer
34 suggests discussing tissue engineering first, then methods for scaffold preparation, followed by 3D
35 culture (paragraph 4), then alginate paragraphs. The introduction needs to be reorganized.”
36
37

38 We have followed the reviewer’s suggestion in reorganizing the introduction which indeed improved
39 the introduction section.
40

41 “For the 3D printing of mesh scaffold, the pore is the space for cell growth to form spheroid. From
42 the top view, the pore is completely empty and the bottom is the surface of 12-well cell culture
43 plate. In this case, the cell can settle down to the bottom and attach to the surface of 12-well cell
44 culture plate. So how the cell can form spheroids? The details need to be clarified.”
45
46

47 We thank Reviewer 1 for bringing up this interesting point that should be better explained.
48 In fact, the scaffold had open pores that communicated with the surface of cell culture plate.
49 However, while the scaffold was coated with gelatin 0.2% at the end of its preparation, the culture
50 plates were not, and after coating and seeding the scaffold was removed and plated in a new cell
51 culture plate. We still could observe cells in the cell culture plate but in fact, many of them remained
52 in the scaffold and formed spheroids as can be seen in the figures along the manuscript.
53
54

55 “The hydrogel is prepared with gelatin and the percentage is much higher than alginate, why further
56 gelatin coating is performed for cell attachment? Since gelatin can support cell attachment, single
57 cell can attach to the hydrogel, how the cells form spheroids on a cell attachable hydrogel? The
58 mechanism for spheroid formation needs to be further discussed.”
59
60

1
2
3 We thank Reviewer 1 for the opportunity of discussing this interesting aspect. In fact, we were
4 surprised by the results obtained. We expected to see cells colonizing the scaffold as described by
5 Pan T et al. (Pan T, Song W, Cao X, Wang Y. 3D Bioplotting of Gelatin/Alginate Scaffolds for Tissue
6 Engineering: Influence of Crosslinking Degree and Pore Architecture on Physicochemical Properties. J
7 Mater Sci Technol. 2016;32(9)) for a similar hydrogel (20% gelatin/4% alginate hydrogel), although
8 these authors used different cells. However, keratinocytes organized into spheroids.

9
10 We tried several percentages of alginate and gelatin in order to obtain scaffolds with desirable
11 stability and mechanical properties and simultaneously with characteristics that promote cell
12 adhesion and growth. Even being the gelatin percentage higher, when we mixed alginate with
13 gelatin before using this mixture to print the scaffold, we could not guarantee that gelatin was at the
14 superficial part of the scaffold, after printing. Also, as the cells were not incorporated into the
15 scaffold during printing but seeded after the printing, this could be a sensitive issue. So, we tried to
16 do a coating of the scaffold with 0.2% gelatin solution because at the beginning of the experiment's
17 cells did not seem to be fixing on the scaffold. In fact, as we described, at these conditions' cells
18 formed spheroids. We discussed this in Discussion section:

19
20 "Although we tried to promote the adhesion of cells to the scaffold using a large proportion of
21 gelatin in our hydrogel and using a 0.2% gelatin coating, cell-cell interactions seemed stronger,
22 showing the predominant spheroid formation and only a few isolated cells growing along the
23 scaffold"-Discussion Section, page 14-15.

24 Similar results were obtained for keratinocytes although for a different matrix (Nie Y, Xu X, Wang W,
25 Ma N, Lendlein A. Spheroid formation of human keratinocyte: Balancing between cell-substrate and
26 cell-cell interaction. In: Clinical Hemorheology and Microcirculation. 2020).

27 Also, the methodology to ensure scaffold sterilization may have changed gelatin structure or
28 properties.

29
30
31 "The core of spheroid is becoming smaller and the surrounding is becoming bigger over time, the
32 reason of this results should be further discussed."

33
34
35 "If the size of spheroids can be adjusted and how it can be adjusted? In addition, a graph is
36 suggested to show the change of spheroid size over time as well as the size of core and surrounding
37 cells."

38
39 In fact, as referred by Reviewer 1 and can be seen in figure 4, not only the core of spheroid is
40 becoming smaller and the surrounding is becoming bigger over time, but the overall size of the
41 spheroid is increasing. The MTT assay showed that not only the cells at the core of the spheroid, but
42 the cells of the entire spheroid are viable. Also, the results obtained for F-actin, involved in cell
43 division and migration showed that cells in the spheroids are active and interacting with each other.
44 This suggests that cells are viable and proliferation, occupying all the space of the pore after 7 days.
45 This is discussed in the Discussion section, page 17, we propose that "our scaffolds promoted
46 spheroid formation and growth. About 47% of all the pores were filled with a spheroid on day 3 and
47 45% on day 7. Spheroids were significantly larger over one week, showing a growth of about 21%
48 between days 3 and 7, filling a more significant portion of each pore. This indicates that the cells
49 inside these spheroids are viable and in proliferation. "

50
51 Our results suggest that spheroid size could be adjusted by changing spheroid pore size, although
52 this needs further confirmation.

53 We thank Reviewer 1 for the suggestion to improve the graph of Figure 3b), with spheroid size over
54 time as well as the size of core and surrounding cells, which we followed as can be seen in the new
55 Figure 3b).-
56

57
58 "The hydrogel shows good compatibility to cells and the cell viability is high. The cell-cell and cell-

1
2
3 ECM interactions affects proliferation, how is the cell proliferation over time? Quantification of cell
4 number is recommended.”

5
6 The authors thank Reviewer 1 for bringing this question.

7 We tried to evaluate the proliferation capacity of the cells in the spheroid with anti-Ki-67-Alexa Fluor
8 labeling. However, the images obtained seemed to have too much non-specific labelling which we
9 were not able to improve in order to obtain an unequivocal measurement. So, although they might
10 suggest a proliferative state, we did not include this evaluation. Nevertheless, the results obtained
11 for MTT assay, indicating mitochondria activity, for F-actin, a molecule involved in cell
12 division and migration of cells (as discussed above), as well as the images obtained for spheroids in
13 which it can be seen an increase in spheroid volume strongly suggest that the cells are in a
14 proliferative state.
15

16
17
18 “The citation of references is messy, please reorganize it and present references in order.”

19
20 The authors thank Reviewer 1 for this observation. The citations reference was already corrected.

21
22 “Figure 2c, three colors are used for 3 time points, the color for legend of E1/E2 is the same as day0.
23 To avoid confusion, black color for legend of E1/E2 is suggested.”

24
25 The authors thank Reviewer 1 for this pertinent commentary and corrected as suggested.
26
27
28
29
30

31 Reviewer: 2

32
33
34 “Rocha et al reported an interesting work in their manuscript titled “A 3D printed hydrogel to
35 promote human keratinocytes spheroid-based growth”. This manuscript can be accepted for
36 publication after a revision.”

37
38
39 “ Authors are advised to correct the linguist errors, especially in the abstract and introduction.
40 Sentence structure and readability need to be improved.”

41
42 The authors thank Reviewer 2 for the kindly comments that helped authors to improve text and
43 correct linguist errors and we hope that now the manuscript is significantly improved and meet the
44 high journal standards.
45

46
47 “It will be interesting to discuss the major characteristics of bioengineered skin substitutes or tissue-
48 engineered skin based on the
49 articles <https://doi.org/10.1080/00914037.2014.977900>, <https://doi.org/10.1038/nbt.1503> in the
50 introduction.”

51
52 As suggested by Reviewer 2, the authors introduced the issues discussed in these two articles in the
53 manuscript.

54 Please see in Introduction section, page 6, the following paragraph:

55 “Interestingly enough, Aasen T et al., (<https://doi.org/10.1038/nbt.1503>) reprogrammed
56 keratinocytes from human skin biopsies and single human hairs to pluripotency cells, that then
57 differentiate again forming a stratified epidermis in 7 days, developing a very interesting model for
58 tissue reepithelization that deserve to be explored for patient-specific therapy.”
59
60

1
2
3 And in Discussion section, page 23:

4 "Other sterilization processes that do not induce significant changes in the properties of the
5 scaffolds have been suggested by Augustine et al.,
6 (<https://doi.org/10.1080/00914037.2014.977900>). The sterilization by gamma radiation above 35
7 kGy of polycaprolactone scaffolds eliminated the presence of microorganisms and did not modify
8 fibroblasts growth, proliferation and adhesion to the scaffold. On contrary, cells seem to grow better
9 on gamma radiation sterilized material."
10
11
12

13 "The last paragraph of the introduction should include a one-sentence conclusion of background
14 information about the study, the hypothesis in one or two sentences, and the experimental
15 strategies and expected outcomes."
16
17

18 We followed this pertinent comment from the Reviewer 2 and added the relevant information in the
19 introduction.
20

21 "Authors mentioned the porosity of the scaffolds however, the measurement just based on the
22 spheroid is not alone a good approach for that. Authors are advised to perform porosity
23 measurements of dry scaffolds (without or with cells) using a simple alcohol diffusion method. The
24 method can be obtained from the article <https://doi.org/10.1007/s12274-017-1549-8>"
25
26
27

28 The authors thank Reviewer 2 for the opportunity of clarifying this issue. In fact, the term "porosity"
29 is referred 3 times along the text as a property of the scaffold matrix important for its properties:

30 -"Different methods have been described to create scaffolds. For example, computer-assisted
31 design (CAD) and manufacturing (CAM) techniques allow more precise control of porosity and
32 shape"
33

34 -"Different properties like structure, porosity, and biodegradability can influence cell growth [12]"

35 -"The G-code used for printing was automatically generated by a python script, allowing to easily
36 adjust all scaffold measurements and precise control of porosity and shape"
37

38 Nevertheless, the measurement of porosity was out of the scope of this work.

39 We think the measurement that Reviewer 2 refers to, based on the spheroid dimensions, is not in
40 fact the measurement of scaffold porosity but the measurement of what we refereed many times
41 along the text as "pore" or "pore size" which is not related to the porosity referred above, but to the
42 size of the "holes" of the scaffold. Other authors also used this terminology and we defined it at the
43 beginning of the manuscript:

44 "The line width was set to 350 μm , and the distance between each printed line was set to 500 μm
45 and will be referred to as "pore" from now on (Fig. 1b)" as can be seen in Materials and Methods - 1.
46 Hydrogel preparation and scaffold printing.

47 To avoid misunderstanding we included a new reference to this on the Materials and Methods
48 section - 3. Scaffold pore size.

49 "The term pore used along the manuscript does not refer to the porosity of the scaffold matrix but
50 to the "holes" of the scaffold. During the scaffold printing the line width was set to 350 μm , and the
51 distance between each printed line was set to 500 μm and is referred to as "pore" along the
52 manuscript."
53
54
55
56
57
58
59
60

1. Title page

A 3D printed hydrogel to promote human keratinocytes' spheroid-based growth

Running head- 3D printed hydrogel to promote keratinocytes spheroids

Tânia Rocha^{1*}, Ana Margarida Teixeira^{2,3}, Susana G. Gomes^{5,6,7}, António André^{2,3}, Pedro Martins^{3,4}, João Ferreira^{2,3*†}, Rita Negrão^{1,8*}

1-Department of Biomedicine, Biochemistry Unit, Faculty of Medicine, University of Porto, 4200-319 Porto, Portugal;

2-Department of Mechanical Engineering, Faculty of Engineering, University of Porto, 4200-465 Porto, Portugal;

3- Institute of Science and Innovation in Mechanical and Industrial Engineering, 4200-465 Porto, Portugal;

4- Aragonese Foundation for Research and Development (ARAID), Aragón Institute of Engineering Research (i3A), University of Zaragoza, Aragón, Spain;

5-Institute for Research and Innovation in Health (i3S), University of Porto, 4200-135 Porto, Portugal;

6-Institute of Molecular Pathology and Immunology of the University of Porto-IPATIMUP, 4200-135 Porto, Portugal;

7 -Faculty of Nutrition and Food Sciences, University of Porto, 4150-180 Porto, Portugal;

8- CINTESIS @ RISE - Center for Health Technology and Services Research, 4200-319 Porto, Portugal.

*These authors contributed equally to the work

†Corresponding author:

Name: João Pedro Sousa Ferreira

Address: Rua Dr Roberto Frias, 4200-465, Porto

Telephone: +351225081400

FAX: +351225081400

Email: j.ferreira@fe.up.pt

Email: j.ferreira@fe.up.pt

Work done in:

1. Title page

Department of Biomedicine, Faculty of Medicine, University of Porto - Alameda Prof. Hernâni Monteiro, 4200-319 Porto, Portugal; And Institute of Science and Innovation in Mechanical and Industrial Engineering - Rua Dr. Roberto Frias 400, 4200-465 Porto, Portugal

For Peer Review

2. Abstract and key terms

Abstract

Tissue engineering uses cells and biomaterials to develop bioartificial tissue substitutes for different purposes. ~~Although~~For example, although several skin models have been developed for pharmaceutical and cosmetic research and skin wound healing, there are few studies on 3D cultures of keratinocytes in 3D printed scaffolds.

So, this work aimed to develop a 3D-printed hydrogel scaffold to promote human keratinocyte growth. Mesh 3D scaffolds were printed using an extrusion-based method with a 20% gelatin/ 5% alginate hydrogel, where HaCaT cells were cultured for seven days.

Scaffolds kept their structure for over one week, and their stiffness only decreased after seven days, showing good mechanical and structural characteristics and ~~good~~ biodegradability (27% weight lost). Viable keratinocytes (MTT assay) are aggregated into spheroids, a 3D model capable of mimicking in vivo ~~cells~~cell properties and phenotypes. Spheroids were formed on 47% of scaffolds pores and grew over time, showing promising cell proliferation. F-actin staining showed cells' irregular and interconnected shapes and organization over time.

This method offers an easy and inexpensive solution for keratinocyte spheroid formation, which may be helpful in tissue engineering as a cell delivery system, for pharmacological or basic research, or ~~for~~ wound healing medical applications.

Key terms: Tissue engineering, biomaterials, alginate, gelatin, skin, regeneration, wound healing, HaCaT

3. Introduction

Introduction

Tissue engineering is a biomedical engineering field that combines cells and biomaterials to replace or regenerate tissues³. Biomaterials can be used to reconstruct damaged tissue, in wound healing, and as a cell or drug delivery system^{9,16}. However, as tissues have different architectural structures and extracellular matrix (ECM) properties, biomaterials should mimic the characteristics of these tissues, allowing cell attachment, migration, proliferation, and enabling the diffusion of nutrients and waste products^{3,9}.

Alginate is a natural biomaterial investigated for biomedical applications due to its biocompatibility, low toxicity, and crosslinking ability by adding divalent cations such as Ca^{2+} ¹⁶. However, alginate lacks cell adhesive ligands, so it is often mixed with other biomaterials, such as gelatin, to improve cell adhesion and differentiation²⁸.

Alginate has also been used for many years as a dressing for highly exuding wounds, ulcers, surgical incisions, and infected wounds¹. Some commercially available solutions include AlgiCell™ (Derma Sciences), AlgiSite M™ (Smith & Nephew), and Tegagen™ (3M Healthcare)¹⁶. These dressings are helpful because they create a moist wound environment, are highly absorptive, nonadherent, biodegradable, and can prevent microbial contamination¹. The application of alginates to skin graft donor sites also results in significantly better healing and reduced pain compared to paraffin gauze controls². Gelatin can also stimulate cell differentiation and proliferation and promote wound healing¹⁸.

3D cell culture systems have been extensively studied, especially in tissue engineering, because cellular properties and phenotypes are closer to those observed in vivo when compared to 2D cell culture systems⁴. Organoids and spheroids are 3D cell culture models where cells grow in complex systems closest to physiological and pathological ones and are of great interest and potential in disease models and regenerative medicine⁴.

Tissue engineering often involves scaffolds where cells are seeded, and their growth stimulated to form viable and functional tissues for medical purposes^{3,9}, like skin¹², bone, or cartilage regeneration⁴. It has also been used to design in vitro models of healthy or pathological tissues and organs for cosmetic and drug tests, the evaluation of new therapies as well as the investigation of phenomena regulating disease onset and progression³. For

3. Introduction

example, there are skin models for psoriasis (TESTSKIN™), melanoma, and even infection models¹².

Different methods have been described to create scaffolds. For example, computer-assisted design (CAD) and manufacturing (CAM) techniques allow more precise control of porosity and shape. They are fast and reproducible compared to conventional methods like gas foaming, melt molding, and freeze-drying techniques⁹. The scaffolds can be created using extrusion-based printing, fused deposition modeling, or selective laser sintering¹³. Extrusion-based systems print the biomaterial layer by layer through a micro-nozzle in the form of continuous filaments through continuous extrusion force¹³. Different biomaterials can be used for this purpose. However, hydrogels are attractive options because their mechanical properties can be adjusted, they are biocompatible, and can be hydrated, similarly to biological tissues, while remaining insoluble and maintaining their 3D structure¹⁰. Hydrogels are matrixes of hydrophilic polymers that absorb large amounts of water, facilitating the transport of nutrients and oxygen and removing waste products. They also present bioactive stimuli that can influence cellular processes¹⁰.

Different properties like structure, porosity, and biodegradability can influence cell growth²¹, so it is essential to study and design new scaffolds and biomaterials to sustain these 3D cell culture systems.

The skin is the largest organ of the human body and has a fundamental role as a protective barrier and immune organ. It also plays a vital role in body temperature regulation and perception of stimuli.

The epidermis is the outermost layer of the skin, and keratinocytes, the predominant cells in this skin layer, are responsible for the production of keratin used as a protective skin barrier. They have an essential role in wound healing re-epithelialization processes^{15,23} and can increase their replication rate during inflammation, disease, or injury³¹. When the skin is damaged, it is essential to repair and restore its functions and prevent complications¹⁹.

Although several skin models have been developed like Skinethic™, Episkin™, and Epiderm™ for both in vivo and in vitro applications for wound healing, disease models, and pharmacological and basic research⁹, there are still few studies on 3D cultures of keratinocytes in 3D-printed scaffolds.

3. Introduction

1
2
3 So, this work aimed to develop a 3D-printed hydrogel scaffold able to promote the growth of
4 human keratinocytes.
5
6
7
8
9
10
11
12
13
14
15
16
17
18
19
20
21
22
23
24
25
26
27
28
29
30
31
32
33
34
35
36
37
38
39
40
41
42
43
44
45
46
47
48
49
50
51
52
53
54
55
56
57
58
59
60

For Peer Review

3. Introduction

Tissue engineering is a biomedical engineering field that combines cells and biomaterials to replace or regenerate tissues [1]. Biomaterials can be used to reconstruct damaged tissue, in wound healing, and as a cell or drug delivery system [2,3]. However, as tissues have different architectural structures and extracellular matrix (ECM) properties, biomaterials should mimic the characteristics of these tissues, allowing cell attachment, migration and proliferation, and enabling the diffusion of nutrients and waste products [1,2]. Tissue engineering often involves scaffolds where cells are seeded and their growth stimulation to form viable and functional tissues for medical purposes [1,2], like skin [4], bone, or cartilage regeneration [5]. It has also been used to design in vitro models of healthy or pathological tissues and organs for cosmetic and drug tests, to evaluate new therapies and investigate phenomena regulating disease onset and progression [1]. For example, there are skin models for psoriasis (TESTSKIN™), melanoma and infection [4].

3D cell culture systems have been extensively studied, especially in tissue engineering, because cellular properties and phenotypes are closer to those observed in vivo when compared to 2D cell culture systems [5]. Organoids and spheroids are 3D cell culture models where cells grow in complex systems closest to physiological and pathological ones and are of great interest and potential in disease models and regenerative medicine [5]. Interestingly enough, Aasen T et al., [6] reprogrammed keratinocytes from human skin biopsies and single human hairs to pluripotency cells, that then differentiate again forming a stratified epidermis in 7 days, developing a very interesting model for tissue reepithelization that deserve to be explored for patient-specific therapy. Alginate is a natural biomaterial for biomedical applications due to its biocompatibility, low toxicity, and crosslinking ability by adding divalent cations such as Ca^{2+} [3]. However, alginate lacks cell-adhesive ligands, so it is often mixed with other biomaterials, such as gelatin, to improve cell adhesion and differentiation [7]. Alginate has also been used for many years as a dressing for highly exuding wounds, ulcers, surgical incisions, and infected wounds [8]. Some commercially available solutions include Algicell™ (Derma Sciences), AlgiSite M™ (Smith & Nephew), and Tegagen™ (3M Healthcare)[3]. These dressings are helpful because they create a moist wound environment, are highly absorptive, nonadherent, biodegradable, and can prevent microbial contamination [7]. The application of alginates to skin graft donor sites also results in significantly better healing and reduced

3. Introduction

1
2
3 pain compared to paraffin gauze controls [9]. Gelatin can also stimulate cell differentiation
4 and proliferation and promote wound healing [10].

5
6
7 Different methods have been described to create scaffolds. For example, computer-assisted
8 design (CAD) and manufacturing (CAM) techniques allow more precise control of porosity and
9 shape. They are faster and more reproducible than conventional gas foaming, melt molding,
10 and freeze-drying techniques [2]. The scaffolds can be created using extrusion-based printing,
11 fused deposition modeling, or selective laser sintering [11]. Extrusion-based systems print the
12 biomaterial layer by layer through a micro-nozzle in the form of continuous filaments through
13 continuous extrusion force [11]. Different biomaterials can be used for this purpose.
14 However, hydrogels are attractive options because their mechanical properties can be
15 adjusted, they are biocompatible and they can be hydrated, similarly to biological tissues,
16 while remaining insoluble and maintaining their 3D structure [12]. Hydrogels are matrixes of
17 hydrophilic polymers that absorb large amounts of water, facilitating the transport of
18 nutrients and oxygen and removing waste products. They also present bioactive stimuli that
19 can influence cellular processes [12]. Different properties like structure, porosity, and
20 biodegradability can influence cell growth [13], so it is essential to study and design new
21 scaffolds and biomaterials to sustain these 3D cell culture systems.

22
23
24
25
26
27
28
29
30
31
32
33
34
35 The skin is the largest organ of the human body and has a fundamental role as a protective
36 barrier and immune organ. It also plays a vital role in body temperature regulation and
37 perception of stimuli. The epidermis is the outermost layer of the skin, and keratinocytes, the
38 predominant cells in this skin layer, are responsible for the production of keratin used as a
39 protective skin barrier. They are essential in wound healing re-epithelialization processes
40 [14,15] and can increase their replication rate during inflammation, disease, or injury [16].
41 When the skin is damaged, it is essential to repair and restore its functions and prevent
42 complications [17]. Although several skin models have been developed, like Skinethic™,
43 Episkin™, and Epiderm™, for both in vivo and in vitro applications for wound healing, disease
44 models and pharmacological and basic research [2], there are still few studies on 3D cultures
45 of keratinocytes in 3D printed scaffolds.

46
47
48
49
50
51
52
53
54
55 We hypothesize that human keratinocytes can grow and proliferate in 3D-printed alginate-
56 based scaffolds. To test this hypothesis, we applied MTT and Phalloidin assays on human
57 keratinocytes seeded in these hydrogels, along with the biodegradability evaluation and
58
59
60

3. Introduction

1
2
3 quantification of macroscopic mechanical properties under compression. Our cell viability
4 results show the formation of spheroids and their continuous growth over a week.
5
6 Furthermore, the hydrogel scaffolds had a macroscopic stiffness of the same order of
7 magnitude as skin and sustained their structure over a week.
8
9
10
11
12
13
14
15
16
17
18
19
20
21
22
23
24
25
26
27
28
29
30
31
32
33
34
35
36
37
38
39
40
41
42
43
44
45
46
47
48
49
50
51
52
53
54
55
56
57
58
59
60

For Peer Review

4. Materials and Methods

Materials and Methods

1. Hydrogel preparation and scaffold printing

The hydrogel was a mixture of 20% of gelatin and 5% of alginate, and it was prepared using a previously described method ⁴⁴.[\[18\]](#). Briefly, 2g of gelatin (Merck, Germany) was dissolved in 10 mL of sterile phosphate buffer saline (PBS) at 60°C. Then 0.5g of sodium alginate (MP Biomedicals, Portugal) was added, and the mixture was stirred and heated at 60°C until a uniform solution was obtained. To remove air bubbles, the hydrogel was centrifuged three times at 2600 *g* for 5 min and one more time, if necessary. The hydrogel was reheated at 60°C between each centrifugation. It was then aspirated with a 5 ml syringe (dicoNex, France) and transferred to 3 ml cartridges with an adapter (Cellink, Sweden). Finally, a sterile solution of 50 mM calcium chloride dihydrate (Merck, Germany) was prepared and added to 3 ml cartridges using the same method so that it could also be dispensed at the time of printing. The scaffolds were printed using the INKREDIBLE+ bioprinter (Cellink, Sweden). The G-code used for this printing was automatically generated by a parameterized script written in Python3, allowing rapid iteration and testing. Before starting the printing process, all material was disinfected with 70% ethanol, and the printer airflow was set at maximum speed to avoid potential contamination. The hydrogel-filled cartridge was loaded in the printing head (PH) 1 spot with a 27-gauge (210 μm) nozzle, and it was set at a temperature of 37°C and a pressure of approximately 100 kPa. In the cartridge with the CaCl_2 solution, a 22-gauge nozzle (410 μm) was used, and it was loaded in the PH2 at room temperature and with a pressure of 2 kPa. The scaffolds were then printed onto a 12-well cell culture plate. Each structure consisted of a layer-by-layer printed mesh (Fig. 1), with 15 columns and 15 lines, for a total of 5 layers. The line width was set to 350 μm , and the distance between each printed line was set to 500 μm and will be referred to as "pore" from now on (Fig. 1b). In total, the scaffold side ~~measured had~~ [a size of](#) 12,25mm. As each scaffold was printed, approximately 500 μl of CaCl_2 was dispensed from the second printing head (PH2) over each structure so that the time between the end of the impression and the crosslinking of the scaffold was uniform between all, without the need to open the printer door, therefore avoiding contamination.

4. Materials and Methods

[Figure 1 around here]

2. Scaffold sterilization and coating

The scaffolds were then transferred to a new sterile 12-well plate inside a laminar flow hood, washed with sterile Tris buffer saline solution (TBS, Sigma, Portugal) three times, and sterilized for 20 minutes with UV radiation. In order to create a gelatin coating on the structures and improve cell adhesion, scaffolds were covered with 500 μ l of sterile 0.2% gelatin solution and incubated for 15 min at 37°C. Finally, they were transferred to sterile 24-well plates to maximize the area in contact with the cell suspension and to decrease scaffold oscillations inside the well. Cell seeding was performed in these coated scaffolds.

3. Scaffold pore size

Scaffolds were photographed (Motic AE31E, Spain), and 7 random pores from each day (3rd and 7th day) were chosen. Three pore size measurements were performed on each pore using ImageJ software® (National Institute of Health, USA). During the scaffold printing the line width was set to 350 μ m, and the distance between each printed line was set to 500 μ m and is referred to as "pore" along the manuscript. For simplicity, we also refer "porosity" to the "holes" of the scaffold and not to the porosity of the scaffold matrix.

4. Degradation assay

~~In order to~~To test ~~scaffolds~~scaffold degradation, they were weighed on the day of print (day zero) and the 3rd and 7th days. Scaffold weight loss was calculated in percentage on day 3 and 7, compared to day 0. Between weighings, the scaffolds were maintained in a cell culture medium at 37°C in the cell incubator and dried as much as possible before each weighing (KERN 770, Germany).

5. Mechanical tests

Mechanical tests were conducted at room temperature under displacement control with a flat-ended circular indenter of 5 mm diameter. A 10N S-beam load cell (Applied Measurements, UK), threaded with the indenter, was connected to an actuator with a load capacity of 12 kg and a resolution of 3.05×10^{-4} mm. Both indentation load P and ~~indenter'~~indenter's position z were acquired at 50 Hz. A 0.02 N preload was applied to ensure

4. Materials and Methods

~~full~~complete contact between the surfaces of the sample and the indenter. Before testing, each sample was subjected to 3 preconditioning cycles at 5 mm/min with an amplitude of 0.3 mm to remove any internal stress accumulation that could arise from sample preparation. Then, ten cycles of 1mm at 5mm/min were applied followed by a stress relaxation test of 3min after ramping to 1.5mm at 30 mm/min (Fig. 2a).

The stress and strain values were obtained from the recorded force-position data as $\sigma = P/(\pi a^2)$ and $\varepsilon = (z - z_0)/z_0$, with a being the radius of the loaded area and z_0 is the sample thickness. As flat circular indenter contact a flat surface, a remains constant during contact.

~~The apparent Young's modulus of the hydrogel was then estimated as~~^{6,14,22,25}The apparent Young's modulus of the hydrogel was then estimated as [19–22]

$$E = 2 \frac{a(1 - \nu^2)\sigma}{z_0 \varepsilon},$$

The Poisson's ratio ν was set to 0.5 due to the incompressibility of the hydrogel (high water content). We calculated E in the first (E1) and second (E2) half of each cycle loading curve. For each group (days after printing), the stress-strain curves were averaged using the experimental data from three samples. The mean (per day after printing) stress-strain curve was used to estimate Young's modulus.

6. Keratinocytes cell culture

HaCaT cells (CLS, Germany) were cultured in Dulbecco's Modified Eagles's Medium (DMEM, CLS, Germany) supplemented with 10% fetal bovine serum (FBS, Sigma-Aldrich, Portugal) and 1% penicillin/streptomycin (Sigma-Aldrich, Portugal) (complete DMEM) at 37 °C and 5% CO₂ and collected by trypsinization with 0.25% trypsin-EDTA solution (Sigma-Aldrich, Portugal). The cell medium was changed every three days. 4×10^5 Cells were seeded on each scaffold. The scaffolds with HaCaT cells were maintained in complete DMEM and cell culture conditions for 3 and 7 days. HaCaT cells were also cultured in 24-well plates, without scaffolds, in the same conditions.

7. Viable cell labeling

4. Materials and Methods

To identify viable cells in the scaffold, under microscope observation, the 3-(4,5-dimethylthiazol-2-yl)-2,5-diphenyltetrazolium bromide (MTT, Sigma-Aldrich, Portugal) assay was used. The formation of a purple formazan inside cells indicates the presence of viable cells. ~~At~~On days 3 and 7, the scaffolds were transferred to different 24-wells plates to avoid labeling cells that were not adherent to the scaffold. Then, 500 μ l of cell culture medium and 100 μ l of 5mg/ml MTT were added and cells were incubated at 37°C for 2 hours. After that, scaffolds with HaCaT cells were analyzed and photographed using an inverted optical microscope (Motic AE31E, Spain).

8. Measurement of spheroid size

Spheroids observed after MTT staining were also used for nucleus and total diameter determination at 3rd and 7th days. At least six randomly stained spheroids were photographed (Motic AE31E, Spain), and three diameter measurements were performed on each spheroid using ImageJ software[®] (National Institute of Health, USA).

9. Quantification of spheroid filled pores

The number of pores of the scaffolds occupied with spheroids was compared to the total number of pores in each scaffold, which was 196 in total (%). Spheroids were easily observed as white spots present in the scaffolds. Therefore, scaffolds with a minimum of 8 white spots per quadrant were selected for quantification. The spheroids were counted ~~directly on the scaffold in the cell culture plate~~days 3 and 7 using an inverted optical microscope (Nikon ECLIPSE 50i, UK). ~~Two time points were compared, the 3rd and 7th days of cell culture.~~

11. Cytoskeleton labeling

Actin filaments (F-actin) from the cytoskeleton of HaCaT cells growing on scaffolds were ~~labelled~~labeled with Alexa Fluor™ 488 Phalloidin A12379 (Invitrogen, Thermofisher, Portugal), at the 3rd and 7th days of cell culture.

HaCaT cells were also seeded on glass coverslips, previously coated with 0.2% gelatin, in 24-well plates, as a control of 2D culture growth.

Briefly, cells were fixed in 4% paraformaldehyde in TBS for 10 minutes at room temperature, rinsed with TBS and then cells were stained by incubation with Alexa Fluor™ 488 Phalloidin

4. Materials and Methods

A12379 in 1% BSA for 20 min, rinsed ~~3~~three times quickly in TBS and mounted in glycerol:PBS to the cover slip. Cells were also stained with 1 $\mu\text{g}/\text{ml}$ 4',6-Diamidine-2'-phenylindole dihydrochloride (DAPI, Roche, Portugal) for 10 min, at room temperature. Images were examined and captured under a fluorescence microscope (Zeiss Axio Imager Z1, Carl Zeiss, Germany) with 495 nm (Alexa Fluor™ 488) and 340/380 nm (DAPI) excitation filters and processed with the Carl Zeiss™ AxioVision program version 4.8.

12. Calculations and statistics

Data are expressed as arithmetic mean \pm standard deviation (SD) except for indentation values E1 and E2 where ~~standard error of the mean (SEM) was used. For comparisons between two groups, Welch's t test was used. Differences were considered significant, at a confidence interval of 95%, whenever $p < 0.05$ and the following symbols were used to mark significance levels: $p^* < 0.05$, $p^{**} < 0.01$, $p^{***} < 0.001$. The sample size (n) corresponds to the number of independent measurements. All the statistical analysis was performed in Python using NumPy, Pandas, SciPy and Seaborn packages^{29,30}.~~

4. Materials and Methods

1
2
3 the standard error of the mean (SEM) was used. Welch's t-test was used for comparisons
4 between the two groups. Differences were considered significant at a confidence interval of
5 95% whenever $p < 0.05$, and the following symbols were used to mark significance levels:
6 $p < 0.05$, $p < 0.01$, $p < 0.001$. The sample size (n) corresponds to the number of
7 independent measurements. All the statistical analysis was performed in Python using
8 NumPy, Pandas, SciPy, and Seaborn packages [23,24].
9
10
11
12
13
14
15
16
17
18
19
20
21
22
23
24
25
26
27
28
29
30
31
32
33
34
35
36
37
38
39
40
41
42
43
44
45
46
47
48
49
50
51
52
53
54
55
56
57
58
59
60

For Peer Review

5. Results

Results

Scaffold properties

The structural and mechanical properties of the scaffolds were evaluated. The mean scaffold pore size was $444 \pm 25 \mu\text{m}$ ($n=7$) on day 3 and $443 \pm 47 \mu\text{m}$ ($n=7$) on day 7.

Printed scaffolds were maintained in cell culture conditions for a maximum of 7 days, and their properties were evaluated at on days 3 and 7. All tested scaffolds lost weight during the week. The loss was $23 \pm 2 \%$ ($n=12$, $p=0.0008$) at day 3 and $27 \pm 3 \%$ ($n=12$, $p=0.001$) after 7 days when comparing to day 0 (Fig. 2b). No significant differences in weight loss between day 3 and day 7 were found ($p=0.176$).

Regarding mechanical properties, E1 characterizes the stiffness for low compressive strains, while E2 describes higher strain values. The indentation tests showed that E1 was significantly higher in day 0 ($22 \pm 2 \text{ kPa}$, $n=2$) when compared to day 7 ($10 \pm 2 \text{ kPa}$, $n=4$) ($p=0.031$, Fig.2c) and in day 3 ($17 \pm 1 \text{ kPa}$, $n=3$) when compared to day 7 ($p=0.014$). No significant differences were found between day 0 and day 3 ($p=0.162$). The obtained E2 value was $33 \pm 2 \text{ kPa}$ ($n=2$) at day 0, $26 \pm 3 \text{ kPa}$ ($n=3$) at day 3, and $21 \pm 5 \text{ kPa}$ ($n=4$) at day 7 (Fig.2c). Although E2 results have a similar profile, tending to decrease from day 0 to day 7, no significant differences were found between different days.

Scaffold resilience upon deformation was also evaluated by their relaxation/recovery ability: in the relaxation tests. The observed results were $44 \pm 1 \%$ ($n=3$) on day 0, $32 \pm 11 \%$ ($n=3$) on day 3 and $32 \pm 3 \%$ ($n=5$) on day 7 (Fig.2d). Relaxation significantly decreased from day 0 to day 7 ($p=0.0006$, Fig.2d).

[Figure 2 around here]

Spheroid evolution

It was observed that when HaCaT cells were seeded on the scaffolds, they did not grow in a monolayer covering the scaffold structure. Instead, they organized themselves in spheroid structures (Fig. 3 and 4).

5. Results

When compared to the total number of pores in a scaffold, which was 196, the percentage of pores that were occupied by spheroids was 49% ($n=3$) on day 3. This number decreased slightly to 47% ($n=3$) on day 7 (Fig.3a). This decrease was not statistically significant ($p=0.77$).

Spheroid total size significantly increased from day 3 to day 7 ($p=0.01$, Fig.3b) while nucleus size decreased from day 3 to day 7 ($p=0.009$, Fig.3b). On day 3, the average total size was $270 \pm 11 \mu\text{m}$ ($n=7$) and, on day 7, it was $342 \pm 19 \mu\text{m}$ ($n=6$), showing a growth of about $72 \mu\text{m}$. This size difference can also be seen in Fig.3c and Fig.3d. On day 3, the average nucleus size was $150 \pm 6 \mu\text{m}$ ($n=7$) and on day 7 it was $120 \pm 8 \mu\text{m}$ ($n=6$),

Figure 3c shows a scaffold on the 3rd day, with spheroids inside its pores (the red square illustrates the limits of a pore). These spheroids do not fill the entire pore and are not perfectly spherical (Fig.3c and 3e). In contrast, spheroids on day 7 are larger, rounder, and able to fill the entire pore (Fig.3d and 3f).

[Figure 3 around here]

Cell viability

The viability of cells inside these spheroids was evaluated by MTT assay. After incubating the scaffold with MTT, a formazan accumulates inside viable cells, indicated by a purple color as seen in spheroids images shown in figure 4.

Figure 4a, 4c, 4e and 4g show spheroids on day 3 with different magnifications. A spheroid core with intense purple color and cells around it can be seen, also labelled with purple, indicating viable cells. Figure 4b, 4d, 4f and 4h show spheroids on day 7 with different magnifications. The core of the spheroid at day 7 is smaller, although the entire spheroid is larger when comparing to the spheroid at day 3, as already described in figure 3b. Nevertheless, the core and surrounding cells, which are more abundant, are also marked with purple color, indicating viable cells. These figures also show differences in the size and shape of spheroids of the 3rd and 7th day spheroids.

[Figure 4 around here]

5. Results

Cell cytoskeleton

HaCaT cells cultured on gelatin-coated coverglass were labeled using phalloidin (green) and DAPI (blue) and the results obtained at the 3rd (Fig. 5a) and 7th (Fig. 5b) days are shown in figure 5. These images show 2D ~~cells shape~~ cell shapes through F-actin labeling. Cells are not round and quiescent; they show irregular and interconnected shapes.

Spheroids were ~~labelled~~ labeled using the same protocol; the results are also shown in figure 5. Although cells are organized in 3D spheroid structures at both 3rd (Fig. 5c, 5e and 5g) and 7th (Fig. 5d, 5f and 5h) days of culture, as already mentioned above, cells are not quiescent, showing irregular shapes, particularly in the middle of spheroids (Fig. 5c and 5d). Fig. 5g and 5h show the same spheroids from Fig. 5e and 5f, respectively, but in combination with a white light filter to show the scaffold's pore structure. These images also show a core of aggregated cells that form a spherical structure in the middle of the spheroid and many loose cells in the periphery of these 3D structures. This arrangement was seen on the majority of spheroids on both days.

[Figure 5 around here]

6. Discussion

Discussion

The skin is the largest organ in the human body and has fundamental functions as a physical barrier and immune organ. ~~It can be damaged by, for example, cuts, burns, pressure, or chemicals and impaired wound healing can lead to complications such as infections, neuronal damage and pain¹⁹. Tissue engineering can be critical to promote wound healing, especially when the affected area is too large to be treated with conventional techniques¹². Scaffolds are often used since they enable the formation of viable tissues from 3D cell cultures, which can be used as implants to repair or replace damaged tissues⁴.~~ It can be damaged by, for example, cuts, burns, pressure, or chemicals and impaired wound healing can lead to complications such as infections, neuronal damage and pain [17]. Tissue engineering can be critical to promote wound healing, especially when the affected area is too large to be treated with conventional techniques [4]. Scaffolds are often used since they enable the formation of viable tissues from 3D cell cultures, which can be used as implants to repair or replace damaged tissues [5].

~~Our results demonstrate that scaffolds printed with 20% gelatin/5% alginate hydrogel could promote viable growth of keratinocytes into spheroids within 7 days. Such a model allows the study keratinocytes under 3D growing conditions and can potentially be applied as a cheap and fast carrier of keratinocytes for skin lesions treatment. Spheroids are an important 3D cell culture model. They are self-assembling and complex spherical cell aggregates with cell-cell and cell-matrix interactions that mimic in vivo tissues and their physiological activity⁴. 2D cell cultures, where cells grow in a monolayer attached to a plastic or glass surface are the most known and used methods due to their simplicity, low cost and reproducibility^{4,21,27}. 2D cultured cells manifest different behavior and properties comparatively to in vivo cells as they do not mimic their 3D environment. For example, cells cultured two-dimensionally can be stretched, resulting in cytoskeletal rearrangements and artificial polarity which can limit their interactions, presenting physical and physiological differences, modified biochemical profiles, bioactivity and drug resistance^{4,21,27}. In contrast, 3D cell cultures, like spheroids, mimic the geometry of three-dimensional tissues more accurately. Therefore cells present a profile closer to that shown in vivo²¹, having many applications for tissue engineering⁴.~~

6. Discussion

Spheroids can be fabricated using various methods and the same culture medium as 2D cultures. Scaffold-free approaches produce spheroids alone and scaffold approaches, as used in this study⁴. An essential advantage of scaffolds is the mechanical reinforcement provided to the cells⁴.

Although we tried to promote the adhesion of cells to the scaffold using a large proportion of gelatin in our hydrogel and using a 0.2% gelatin coating, cell-cell interactions seemed stronger, showing the predominant spheroid formation and only a few isolated cells growing along the scaffold²⁰, in contrast to results shown in a previous study using a 20% gelatin/4% alginate hydrogel²¹. Our results demonstrate that scaffolds printed with 20% gelatin/5% alginate hydrogel could promote a viable growth of keratinocytes into spheroids within 7 days. Such a model allows the study of keratinocytes under 3D growing conditions and can potentially be applied as a cheap and fast carrier of keratinocytes for skin lesions treatment. Spheroids are an important 3D cell culture model. They are self-assembling and complex spherical cell aggregates with cell-cell and cell-matrix interactions that mimic in vivo tissues and their physiological activity [5]. 2D cell cultures, where cells grow in a monolayer attached to a plastic or glass surface, are the most known and used methods due to their simplicity, low cost, and reproducibility [5,13]. However, 2D cultured cells manifest different behavior and properties than in vivo cells as they do not mimic their 3D environment. For example, cells cultured two-dimensionally can be stretched, resulting in cytoskeletal rearrangements and artificial polarity, limiting their interactions, presenting physical and physiological differences, modified biochemical profiles, bioactivity, and drug resistance [5,13,25]. In contrast, 3D cell cultures, like spheroids, mimic the geometry of three-dimensional tissues more accurately. Therefore cells present a profile closer to that shown in vivo [13], having many applications for tissue engineering[5].

Spheroids can be fabricated using various methods and the same culture medium as 2D cultures. Scaffold-free approaches produce spheroids alone and scaffold approaches, as used in this study [5]. An essential advantage of scaffolds is the mechanical reinforcement provided to the cells [5].

Although we tried to promote the adhesion of cells to the scaffold using a large proportion of gelatin in our hydrogel and using a 0.2% gelatin coating, cell-cell interactions seemed stronger, showing the predominant spheroid formation and only a few isolated cells growing along the scaffold [26], in contrast to results shown in a previous study using a 20% gelatin/4%

6. Discussion

alginate hydrogel [13]. This could be explained by some denature of gelatin structure as it was subjected to high temperatures to avoid contamination during scaffold preparation.

The lack of studies regarding 3D keratinocytes cell cultures using 3D printed scaffolds able to promote cell growth and other desired properties such as cell adherence, migration and interactions turned relevant to develop a 3D-printed hydrogel scaffold able to promote the growth of human keratinocytes.

We used the HaCaT cell line, a non-tumorigenic monoclonal cell line of spontaneously immortalized human keratinocytes, as it has been proposed as a model for the study of keratinocytes functions. They have some advantages compared to fresh human keratinocytes as they are adapted for long-term growth without additional growth factors, exhibit normal morphogenesis and express all significant surface markers and functional keratinocytes activity, retaining the ability to reconstitute a well-structured epidermis after in vivo transplantation⁷. They have some advantages compared to fresh human keratinocytes as they are adapted for long-term growth without additional growth factors, exhibit normal morphogenesis and express all significant surface markers and functional keratinocytes activity, retaining the ability to reconstitute a well-structured epidermis after in vivo transplantation [27].

Scaffolds were produced using a 3D bioprinter (INKREDIBLE+ by CELLINK) as previously described¹³. This device uses a pneumatic-based system to extrude the hydrogel through a thin nozzle, with precise positioning of a moving printing head in X, Y, and Z. This technology is fast, reproducible and highly computer controllable, thus allowing the precise printing of 3D structures. These may be porous grid structures that promote the circulation of nutrients and metabolites³¹, like in this study.

Scaffolds were produced using a 3D bioprinter (INKREDIBLE+ by CELLINK) as previously described [11]. This device uses a pneumatic-based system to extrude the hydrogel through a thin nozzle, with precise positioning of a moving printing head in X, Y, and Z. This technology is fast, reproducible and highly computer controllable, thus allowing the precise printing of 3D structures. These may be porous grid structures that promote the circulation of nutrients and metabolites [16], like in this study.

The G-code used for printing was automatically generated by a python script, allowing to easily adjust all scaffold measurements and precise control of porosity and shape. It also

6. Discussion

enabled printing in multiwell plates and optimizing the printing process, avoiding unnecessary and time-consuming movements.

The printing head temperature was set to 37°C to facilitate hydrogel extrusion. However, we had some printing precision and reproducibility issues, likely because the printer's platform was at room temperature, and we worked with a temperature-sensitive hydrogel. ~~The printer was also under non-sterile conditions, so scaffolds had to be posteriorly sterilized using UV radiation, a method shown to have promising results in terminal sterilization of alginate scaffolds without affecting their mechanical properties²⁶ or dehydrating the scaffolds like ethanol.~~ The printer was also under non-sterile conditions, so scaffolds had to be posteriorly sterilized using UV radiation, a method shown to have promising results in terminal sterilization of alginate scaffolds without affecting their mechanical properties [28] or dehydrating the scaffolds like ethanol. Other sterilization processes that do not induce significant changes in the properties of the scaffolds have been suggested by Augustine et al. [29]. The sterilization by gamma radiation above 35 kGy of polycaprolactone scaffolds eliminated the presence of microorganisms and did not modify fibroblasts growth, proliferation and adhesion to the scaffold. On contrary, cells seem to grow better on gamma radiation sterilized material. We used a hydrogel with 20% gelatin and 5% alginate, similar to a previously tested hydrogel for mouse bone mesenchymal stem cell growth [13]. Both alginate and gelatin promote wound healing [8,10] and this combination has been described for biomedical applications including the skin [7] and has also been attempted because of its chemical similarity to the ECM [13].

~~We used a hydrogel with 20% gelatin and 5% alginate, similar to a previously tested hydrogel for mouse bone mesenchymal stem cell growth²¹. Both alginate and gelatin promote wound healing^{1,18} and this combination has been described for biomedical applications including the skin²⁸ and has also been attempted because of its chemical similarity to the ECM²¹.~~

The printed scaffolds were mesh structures with a total of 196 pores with 500x500 µm each and a diagonal of 707 µm. On images obtained after printing, some pores appeared rounder, so we measured the most significant dimensions of each one, equivalent to their diagonals. The mean scaffold pore size was 444 µm on 3rd day and 443 µm on the 7th day, about 63% of the initially designed size, but it didn't change over 1 week, which shows good structural integrity. Scaffolds decreased their overall size after crosslinking, and the hydrogel lines may have gotten more prominent due to water absorption, explaining the smaller pore size

6. Discussion

1
2
3 compared to the ~~design²¹-design~~ [13].

4
5 The tests to evaluate scaffold structural integrity and properties during one week revealed
6 that scaffolds kept their basic structure and design after one week, as seen on microscopic
7 images, but some of their properties changed. For example, scaffolds lost 23% of their weight
8 on day 3 and 27% on day 7, when maintained in cell culture conditions, suggesting that this
9 loss occurs in the first days as the decrease observed between the 3rd and 7th days was not
10 significant. Furthermore, the degradation after 7 days was similar to previously reported
11 results for a 20% gelatin/4% alginate hydrogel. However, after 3 days in our study, the
12 degradation was approximately twice the value of the previous ~~results²¹-results~~ [13]. Overall,
13 this hydrogel showed good biodegradability, which could be due to its chemical structure, the
14 incubation temperature or the transport processes of various chemicals such as water and
15 ions (H⁺ and OH⁻)~~¹⁷~~. [30].

16
17
18
19
20
21
22
23
24
25 ~~Indentation tests showed a decrease of scaffolds stiffness throughout the week. However,~~
26 ~~the scaffolds stiffness for low compressive strains (E1) only decreased significantly on day 7~~
27 ~~and for higher strain values (E2) the change was not significant, which shows good mechanical~~
28 ~~strength properties. This is a result of scaffold degradation and consequent loss of resistance.~~
29 ~~Scaffolds also showed a low recovery ability with low relaxation values, meaning they have~~
30 ~~low resilience upon deformation, which could be associated with scaffold stiffness³². After 7~~
31 ~~days, their relaxation decreased significantly (12%) compared to the first day, possibly due to~~
32 ~~ionic and covalent crosslinking changes as the scaffolds spent time in the incubator~~
33 ~~conditions⁵.~~

34
35
36
37
38
39
40
41
42 Indentation tests showed a decrease of scaffolds stiffness throughout the week. However, the
43 scaffolds stiffness for low compressive strains (E1) only decreased significantly on day 7 and
44 for higher strain values (E2) the change was not significant, which shows good mechanical
45 strength properties. This is a result of scaffold degradation and consequent loss of resistance.
46 Scaffolds also showed a low recovery ability with low relaxation values, meaning they have
47 low resilience upon deformation, which could be associated with scaffold stiffness [31]. After
48 7 days, their relaxation decreased significantly (12%) compared to the first day, possibly due
49 to ionic and covalent crosslinking changes as the scaffolds spent time in the incubator
50 conditions [32].

51
52
53
54
55
56
57
58 These mechanical and physical evaluation tests were done in scaffolds without cells to
59 facilitate their manipulation. However, this might have changed the results, even if slightly,
60

6. Discussion

as it has been demonstrated that cells may have a role in crosslinking and degradation processes, affecting scaffold ~~properties~~¹⁶. ~~properties~~ [3]. Therefore, in future studies, scaffolds should also be analyzed using different methods like scanning electron microscopy to study their structural characteristics over time.

Our scaffolds promoted spheroid formation and growth. About 47% of all the pores were filled with a spheroid ~~at on~~ day 3 and 45% ~~at on~~ day 7. Spheroids were significantly larger over ~~1one~~ week, showing a growth of about 21% between days 3 and 7, filling a ~~larger~~^{more} ~~significant~~ portion of each pore. This indicates that the cells inside these spheroids are viable and in proliferation, which is extremely important in tissue engineering and ensuring proper cell delivery. ~~In fact,~~ MTT assay proved the presence of viable cells as a purple color inside cells was observed due to the formazan formed in the 3rd and 7th days, as shown in microscopic images. Accordingly, the results obtained for F-actin labeling, a major cytoskeleton component involved in many cellular processes such as cell division and ~~migration~~²⁴, ~~migration~~ [33], showed that cells in the spheroids are not round and quiescent but rather active and interacting. In phalloidin images, we could see a core of aggregated cells and many loose cells. We do not know if these loose cells mean that they are leaving the spheroid to colonize the scaffold structure or if this was an artifact caused by the washing steps required during the staining protocol. Because of this, spheroid size was measured on MTT assay spheroids, where there was minimal handling of the samples. ~~On~~ ~~The imaging was~~ ~~challenging on~~ both MTT and phalloidin methods, ~~the imaging was challenging~~ due to ~~spheroid~~^{the spheroid's} high thickness, ~~which results~~^{resulting} in a light-scattering phenomenon that limits light ~~penetration~~⁸. ~~Therefore, in the future~~^{penetration} [34]. ~~Therefore~~, spheroids sectioning or optical clearing methods could be used ~~in the future~~ to obtain better ~~resolution~~⁸: ~~resolution~~ [34].

Since alginate has been used for many years as a wound dressing and shows ~~great~~^{significant} characteristics capable of improving healing, the results herein presented represent a new step in this field as they show that alginate/gelatin scaffolds are attractive supports able to promote human keratinocytes growth into spheroids, that deserve to be better explored as wound dressings able to deliver keratinocytes to promote wound healing. Also, as keratinocytes grown in these 3D spheroids structures mimic human ~~tissue~~^{tissue} properties more accurately than monolayer cell cultures, they may be helpful to study models, and the exploration of their clinical and regenerative utility seems ~~of~~ great interest. In future studies,

6. Discussion

1
2
3 other cell types, such as fibroblasts, could ~~also~~ be co-cultured to ~~better~~ mimic skin
4 environment and cell interactions and eventually potentiate healing properties even further.
5
6
7
8
9
10
11
12
13
14
15
16
17
18
19
20
21
22
23
24
25
26
27
28
29
30
31
32
33
34
35
36
37
38
39
40
41
42
43
44
45
46
47
48
49
50
51
52
53
54
55
56
57
58
59
60

For Peer Review

7. Acknowledgments

Acknowledgments

National Funds supported this article through FCT - Fundação para a Ciência e a Tecnologia, IP, within CINTESIS, R&D Unit (reference UIDB/4255/2020) and by project CyclicCell - PTDC/EME-APL/1342/2020 financed through FCT/FEDER/MCTES.

We would like to thank Professor António Avelino for [thehis](#) help with microscopic imaging.

The authors declare no conflict of interest.

For Peer Review

8. References

References

1. Aderibigbe, B. A., and B. Buyana. Alginate in Wound Dressings. *Pharmaceutics* 10:42, 2018.
2. Attwood, A. I. Calcium alginate dressing accelerates split skin graft donor site healing. *British Journal of Plastic Surgery* 42:373–379, 1989.
3. Caddeo, S., M. Boffito, and S. Sartori. Tissue Engineering Approaches in the Design of Healthy and Pathological In-Vitro Tissue Models. *Frontiers in Bioengineering and Biotechnology* 5:, 2017.
4. Chae, S., J. Hong, H. Hwangbo, and G. Kim. The utility of biomedical scaffolds laden with spheroids in various tissue engineering applications. *Theranostics* 11:6818–6832, 2021.
5. Charbonier, F., D. Indana, and O. Chaudhuri. Tuning Viscoelasticity in Alginate Hydrogels for 3D Cell Culture Studies. *Current Protocols* 1:e124, 2021.
6. Cheng (Zheng Zhemin), C. M., and Y. T. Cheng. On the initial unloading slope in indentation of elastic-plastic solids by an indenter with an axisymmetric smooth profile. *Appl. Phys. Lett.* 71:2623–2625, 1997.
7. Colombo, I., E. Sangiovanni, R. Maggio, C. Mattozzi, S. Zava, Y. Corbett, M. Fumagalli, C. Carlino, P. A. Corsetto, D. Scaccabarozzi, S. Calvieri, A. Gismondi, D. Taramelli, and M. Dell’Agli. HaCaT Cells as a Reliable In-Vitro Differentiation Model to Dissect the Inflammatory/Repair Response of Human Keratinocytes. *Mediators Inflamm* 2017:7435621, 2017.
8. Costa, E. C., D. N. Silva, A. F. Moreira, and I. J. Correia. Optical clearing methods: An overview of the techniques used for the imaging of 3D spheroids. *Biotechnology and Bioengineering* 116:2742–2763, 2019.

8. References

- 1
2
3
4
5
6
7
8
9
10
11
12
13
14
15
16
17
18
19
20
21
22
23
24
25
26
27
28
29
30
31
32
33
34
35
36
37
38
39
40
41
42
43
44
45
46
47
48
49
50
51
52
53
54
55
56
57
58
59
60
9. Do, A. V., B. Khorsand, S. M. Geary, and A. K. Salem. 3D Printing of Scaffolds for Tissue Regeneration Applications. *Adv Healthc Mater* 4:1742–1762, 2015.
10. El-Sherbiny, I. M., and M. H. Yacoub. Hydrogel scaffolds for tissue engineering: Progress and challenges. *Glob Cardiol Sci Pract* 2013:316–342, 2013.
11. Giuseppe, M. D., N. Law, B. Webb, R. A. Macrae, L. J. Liew, T. B. Sercombe, R. J. Dilley, and B. J. Doyle. Mechanical behaviour of alginate-gelatin hydrogels for 3D bioprinting. *Journal of the Mechanical Behavior of Biomedical Materials* 79:150–157, 2018.
12. Groeber, F., M. Holeiter, M. Hampel, S. Hinderer, and K. Schenke-Layland. Skin tissue engineering—in vivo and in vitro applications. *Adv Drug Deliv Rev* 63:352–366, 2011.
13. Gu, Z., J. Fu, H. Lin, and Y. He. Development of 3D bioprinting: From printing methods to biomedical applications. *Asian Journal of Pharmaceutical Sciences* 15:529–557, 2020.
14. King, R. B. Elastic analysis of some punch problems for a layered medium. *International Journal of Solids and Structures* 23:, 1987.
15. Klicks, J., E. Molitor, T. Fauth, R. Rudolf, and M. Hafner. In vitro skin three-dimensional models and their applications. *Journal of Cellular Biotechnology* 3:21–39, 2017.
16. Lee, K. Y., and D. J. Mooney. Alginate: properties and biomedical applications. *Prog Polym Sci* 37:106–126, 2012.
17. Lyu, J. Schley, B. Loy, D. Lind, C. Hobot, R. Sparer, and D. Untereker. Kinetics and Time-Temperature Equivalence of Polymer Degradation. *Biomacromolecules* 8:2301–2310, 2007.
18. Ndlovu, S. P., K. Ngece, S. Alven, and B. A. Aderibigbe. Gelatin-Based Hybrid Scaffolds: Promising Wound Dressings. *Polymers (Basel)* 13:2959, 2021.
19. Nguyen, A. V., and A. M. Soulika. The Dynamics of the Skin's Immune System. *Int J Mol Sci* 20:1811, 2019.

8. References

- 1
2
3
4
5
6
7
8
9
10
11
12
13
14
15
16
17
18
19
20
21
22
23
24
25
26
27
28
29
30
31
32
33
34
35
36
37
38
39
40
41
42
43
44
45
46
47
48
49
50
51
52
53
54
55
56
57
58
59
60
20. Nie, Y., X. Xu, W. Wang, N. Ma, and A. Lendlein. Spheroid formation of human keratinocyte: Balancing between cell-substrate and cell-cell interaction. *Clin Hemorheol Microcirc* 76:329–340, 2020.
21. Pan, T., W. Song, X. Cao, and Y. Wang. 3D-Bioplotting of Gelatin/Alginate Scaffolds for Tissue Engineering: Influence of Crosslinking Degree and Pore Architecture on Physicochemical Properties. *Journal of Materials Science & Technology* 32:889–900, 2016.
22. Pharr, G. M., W. C. Oliver, and F. R. Brotzen. On the generality of the relationship among contact stiffness, contact area, and elastic modulus during indentation. *Journal of Materials Research* 7:, 1992.
23. Rodrigues, M., N. Kosaric, C. A. Bonham, and G. C. Gurtner. Wound Healing: A Cellular Perspective. *Physiol Rev* 99:665–706, 2019.
24. Small, J., K. Rottner, P. Hahne, and K. I. Anderson. Visualising the actin cytoskeleton. *Microsc Res Tech* 47:3–17, 1999.
25. Sneddon, I. N. The relation between load and penetration in the axisymmetric boussinesq problem for a punch of arbitrary profile. *International Journal of Engineering Science* 3:, 1965.
26. Stoppel, W. L., J. C. White, S. D. Horava, A. C. Henry, S. C. Roberts, and S. R. Bhatia. Terminal sterilization of alginate hydrogels: Efficacy and impact on mechanical properties. *J Biomed Mater Res B Appl Biomater* 102:877–884, 2014.
27. Sun, T., S. Jackson, J. W. Haycock, and S. MacNeil. Culture of skin cells in 3D rather than 2D improves their ability to survive exposure to cytotoxic agents. *Journal of Biotechnology* 122:372–381, 2006.

8. References

- 1
2
3
4
5
6
7
8
9
10
11
12
13
14
15
16
17
18
19
20
21
22
23
24
25
26
27
28
29
30
31
32
33
34
35
36
37
38
39
40
41
42
43
44
45
46
47
48
49
50
51
52
53
54
55
56
57
58
59
60
28. Van Vlierberghe, S., P. Dubruel, and E. Schacht. Biopolymer-based hydrogels as scaffolds for tissue engineering applications: a review. *Biomacromolecules* 12:1387–1408, 2011.
29. Virtanen, P. et al. SciPy 1.0: fundamental algorithms for scientific computing in Python. *Nat Methods* 17:261–272, 2020.
30. van der Walt, S., S. C. Colbert, and G. Varoquaux. The NumPy Array: A Structure for Efficient Numerical Computation. *Computing in Science and Engineering* 13:22–30, 2011.
31. Weng, T., W. Zhang, Y. Xia, P. Wu, M. Yang, R. Jin, S. Xia, J. Wang, C. You, C. Han, and X. Wang. 3D bioprinting for skin tissue engineering: Current status and perspectives. *J Tissue Eng* 12:20417314211028576, 2021.
32. You, F., X. Wu, and X. Chen. 3D printing of porous alginate/gelatin hydrogel scaffolds and their mechanical property characterization. *International Journal of Polymeric Materials and Polymeric Biomaterials* 66:299–306, 2017.

1. [Caddeo S, Boffito M, Sartori S. Tissue engineering approaches in the design of healthy and pathological in vitro tissue models. Vol. 5, Frontiers in Bioengineering and Biotechnology. 2017.](#)
2. [Do AV, Khorsand B, Geary SM, Salem AK. 3D Printing of Scaffolds for Tissue Regeneration Applications. Vol. 4, Advanced Healthcare Materials. 2015.](#)
3. [Lee KY, Mooney DJ. Alginate: Properties and biomedical applications. Vol. 37, Progress in Polymer Science \(Oxford\). 2012.](#)
4. [Groeber F, Holeiter M, Hampel M, Hinderer S, Schenke-Layland K. Skin tissue engineering - In vivo and in vitro applications. Vol. 63, Advanced Drug Delivery Reviews. 2011.](#)
5. [Chae SJ, Hong J, Hwangbo H, Kim GH. The utility of biomedical scaffolds laden with spheroids in various tissue engineering applications. Theranostics. 2021;11\(14\).](#)
6. [Aasen T, Raya A, Barrero MJ, Garreta E, Consiglio A, Gonzalez F, Vassena R, Bilić J, Pekarik V, Tiscornia G, Edel M, Boué S, Belmonte JCI. Efficient and rapid generation of induced pluripotent stem cells from human keratinocytes. Nat Biotechnol. 2008;26\(11\).](#)
7. [Van Vlierberghe S, Dubruel P, Schacht E. Biopolymer-based hydrogels as scaffolds for tissue engineering applications: A review. Vol. 12, Biomacromolecules. 2011.](#)
8. [Aderibigbe BA, Buyana B. Alginate in wound dressings. Vol. 10, Pharmaceutics. 2018.](#)
9. [Attwood AI. Calcium alginate dressing accelerates split skin graft donor site healing. Br J Plast Surg. 1989;42\(4\).](#)
10. [Ndlovu SP, Ngece K, Alven S, Aderibigbe BA. Gelatin-based hybrid scaffolds: Promising wound dressings. Vol. 13, Polymers. 2021.](#)
11. [Gu Z, Fu J, Lin H, He Y. Development of 3D bioprinting: From printing methods to biomedical applications. Vol. 15, Asian Journal of Pharmaceutical Sciences. 2020.](#)
12. [El-Sherbiny IM, Yacoub MH. Hydrogel scaffolds for tissue engineering: Progress and challenges. Glob Cardiol Sci Pract. 2013;2013\(3\).](#)
13. [Pan T, Song W, Cao X, Wang Y. 3D Bioplotting of Gelatin/Alginate Scaffolds for Tissue Engineering: Influence of Crosslinking Degree and Pore Architecture on Physicochemical Properties. J Mater Sci Technol. 2016;32\(9\).](#)
14. [Rodrigues M, Kosaric N, Bonham CA, Gurtner GC. Wound healing: A cellular perspective. Physiol Rev. 2019;99\(1\).](#)
15. [Klicks J, von Molitor E, Ertongur-Fauth T, Rudolf R, Hafner M. In vitro skin three-dimensional models and their applications. J Cell Biotechnol. 2017;3\(1\).](#)
16. [Weng T, Zhang W, Xia Y, Wu P, Yang M, Jin R, Xia S, Wang J, You C, Han C, Wang X. 3D bioprinting for skin tissue engineering: Current status and perspectives. Vol. 12, Journal of Tissue Engineering. 2021.](#)
17. [Nguyen A V., Soulika AM. The dynamics of the skin's immune system. Vol. 20, International Journal of Molecular Sciences. 2019.](#)
18. [Giuseppe M Di, Law N, Webb B, A. Macrae R, Liew LJ, Sercombe TB, Dilley RJ, Doyle](#)

- 1
2
3 BJ. Mechanical behaviour of alginate-gelatin hydrogels for 3D bioprinting. J Mech
4 Behav Biomed Mater. 2018;79.
5
- 6 19. Cheng CM, Cheng YT. On the initial unloading slope in indentation of elastic-plastic
7 solids by an indenter with an axisymmetric smooth profile. Appl Phys Lett.
8 1997;71(18).
9
- 10 20. King RB. Elastic analysis of some punch problems for a layered medium. Int J Solids
11 Struct. 1987;23(12).
12
- 13 21. Oliver WC, Brotzen FR. On the generality of the relationship among contact stiffness,
14 contact area, and elastic modulus during indentation. J Mater Res. 1992;7(3).
15
- 16 22. Sneddon IN. The relation between load and penetration in the axisymmetric
17 boussinesq problem for a punch of arbitrary profile. Int J Eng Sci [Internet]. 1965 May
18 1;3(1):47–57. Available from:
19 <https://linkinghub.elsevier.com/retrieve/pii/0020722565900194>
20
- 21 23. Virtanen P, Gommers R, Oliphant TE, Haberland M, Reddy T, Cournapeau D, Burovski
22 E, Peterson P, Weckesser W, Bright J, van der Walt SJ, Brett M, Wilson J, Millman KJ,
23 Mayorov N, Nelson ARJ, Jones E, Kern R, Larson E, Carey CJ, Polat İ, Feng Y, Moore
24 EW, VanderPlas J, Laxalde D, Perktold J, Cimrman R, Henriksen I, Quintero EA, Harris
25 CR, Archibald AM, Ribeiro AH, Pedregosa F, van Mulbregt P, Vijaykumar A, Bardelli A
26 Pietro, Rothberg A, Hilboll A, Kloeckner A, Scopatz A, Lee A, Rokem A, Woods CN,
27 Fulton C, Masson C, Häggström C, Fitzgerald C, Nicholson DA, Hagen DR, Pasechnik D
28 V., Olivetti E, Martin E, Wieser E, Silva F, Lenders F, Wilhelm F, Young G, Price GA,
29 Ingold GL, Allen GE, Lee GR, Audren H, Probst I, Dietrich JP, Silterra J, Webber JT,
30 Slavič J, Nothman J, Buchner J, Kulick J, Schönberger JL, de Miranda Cardoso JV,
31 Reimer J, Harrington J, Rodríguez JLC, Nunez-Iglesias J, Kuczynski J, Tritz K, Thoma M,
32 Newville M, Kümmerer M, Bolingbroke M, Tartre M, Pak M, Smith NJ, Nowaczyk N,
33 Shebanov N, Pavlyk O, Brodtkorb PA, Lee P, McGibbon RT, Feldbauer R, Lewis S,
34 Tygiel S, Sievert S, Vigna S, Peterson S, More S, Pudlik T, Oshima T, Pingel TJ,
35 Robitaille TP, Spura T, Jones TR, Cera T, Leslie T, Zito T, Krauss T, Upadhyay U,
36 Halchenko YO, Vázquez-Baeza Y. SciPy 1.0: fundamental algorithms for scientific
37 computing in Python. Nat Methods. 2020;17(3).
38
- 39 24. Van Der Walt S, Colbert SC, Varoquaux G. The NumPy array: A structure for efficient
40 numerical computation. Comput Sci Eng. 2011;13(2).
41
- 42 25. Sun T, Jackson S, Haycock JW, MacNeil S. Culture of skin cells in 3D rather than 2D
43 improves their ability to survive exposure to cytotoxic agents. J Biotechnol.
44 2006;122(3).
45
- 46 26. Nie Y, Xu X, Wang W, Ma N, Lendlein A. Spheroid formation of human keratinocyte:
47 Balancing between cell-substrate and cell-cell interaction. In: Clinical Hemorheology
48 and Microcirculation. 2020.
49
- 50 27. Colombo I, Sangiovanni E, Maggio R, Mattozzi C, Zava S, Corbett Y, Fumagalli M,
51 Carlino C, Corsetto PA, Scaccabarozzi D, Calvieri S, Gismondi A, Taramelli D, Dell'Agli
52 M. HaCaT Cells as a Reliable in Vitro Differentiation Model to Dissect the
53 Inflammatory/Repair Response of Human Keratinocytes. Mediators Inflamm.
54 2017;2017.
55
56
57
58
59
60

- 1
 - 2
 - 3
 - 4
 - 5
 - 6
 - 7
 - 8
 - 9
 - 10
 - 11
 - 12
 - 13
 - 14
 - 15
 - 16
 - 17
 - 18
 - 19
 - 20
 - 21
 - 22
 - 23
 - 24
 - 25
 - 26
 - 27
 - 28
 - 29
 - 30
 - 31
 - 32
 - 33
 - 34
 - 35
 - 36
 - 37
 - 38
 - 39
 - 40
 - 41
 - 42
 - 43
 - 44
 - 45
 - 46
 - 47
 - 48
 - 49
 - 50
 - 51
 - 52
 - 53
 - 54
 - 55
 - 56
 - 57
 - 58
 - 59
 - 60
28. [Stoppel WL, White JC, Horava SD, Henry AC, Roberts SC, Bhatia SR. Terminal sterilization of alginate hydrogels: Efficacy and impact on mechanical properties. J Biomed Mater Res - Part B Appl Biomater. 2014;102\(4\).](#)
29. [Augustine R, Saha A, Jayachandran VP, Thomas S, Kalarikkal N. Dose-dependent effects of gamma irradiation on the materials properties and cell proliferation of electrospun polycaprolactone tissue engineering scaffolds. Int J Polym Mater Polym Biomater. 2015;64\(10\).](#)
30. [Lyu SP, Schley J, Loy B, Lind D, Hobot C, Sparer R, Untereker D. Kinetics and time-temperature equivalence of polymer degradation. Biomacromolecules. 2007;8\(7\).](#)
31. [You F, Wu X, Chen X. 3D printing of porous alginate/gelatin hydrogel scaffolds and their mechanical property characterization. Int J Polym Mater Polym Biomater. 2017;66\(6\).](#)
32. [Charbonier F, Indana D, Chaudhuri O. Tuning Viscoelasticity in Alginate Hydrogels for 3D Cell Culture Studies. Curr Protoc. 2021;1\(5\).](#)
33. [Small JV, Rottner K, Hahne P, Anderson KI. Visualising the actin cytoskeleton. Microsc Res Tech. 1999;47\(1\).](#)
34. [Costa EC, Silva DN, Moreira AF, Correia IJ. Optical clearing methods: An overview of the techniques used for the imaging of 3D spheroids. Vol. 116, Biotechnology and Bioengineering. 2019.](#)

FIGURE CAPTIONS:

Fig. 1 - Scaffold 3D model. (a) Isometric view; (b) Top view; the red square illustrates a pore, the line width is 350 μm and the pore width is 500 μm . Scaffolds size was 12,25 x 12,25 mm^2

Fig. 2 - Scaffolds physical and mechanical properties evaluation (a) Mechanical tests protocol; (b) Scaffold weight loss (%), $p^{***}=0.0008$ when comparing day 0 to day 3 and $p^{**}=0.001$ when comparing day 0 to day 7; (c) Scaffold stiffness (kPa), E1 characterizes the scaffold stiffness for low compressive strains while E2 is for higher strain values, $p^*=0.031$ when comparing E1 day 0 to day 7 and $p^*=0.014$ when comparing E1 from day 3 to day 7; (d) Scaffold relaxation (%), $p^{***}=0.0006$ when comparing day 0 and 7.

Fig. 3 - Cells organized in spheroids in scaffold pores. (a) Spheroid-filled pores (%) on 3rd and 7th days; (b) Spheroid Nucleus and spheroid size (μm) on 3rd and 7th days; (c) Scaffold with spheroid-filled pores on 3rd day and (d) on 7th day (The red square illustrates an entire pore; magnification is 40x); (e) Spheroid inside a pore on 3rd day and (f) on 7th day (magnification is 100x).

Fig. 4 – Evaluation of viability of spheroids cells by MTT labeling (a)(c) Spheroid on 3rd day and (b,d) 7th day with 200x magnification; (e,g) Spheroid on 3rd and (f,h) 7th day with 400x magnification;

Fig. 5 – Immunofluorescence observed upon labeling of HaCaT cells and spheroids with phalloidin (green) and DAPI (blue). (a) 2D cell culture on 3rd day and (b) on 7th day; (c) 3rd day spheroid and (d) 7th day spheroid; (e) Spheroid showing a core of cells surrounded by loose cells on 3rd day and (f) on 7th day; (g,h) the same spheroid as seen in Fig.5e and Fig.5f respectively, but photographed with white light, showing the pore's structure. Magnification of 400x in (a) and (b) and 100x on the remaining images.